NASA Contractor Report 4162

Acousto-Ultrasonic Input-Output Characterization of Unidirectional Fiber Composite Plate by P Waves

Peter Liao and James H. Williams, Jr.

GRANT NAG3-328
JULY 1988

NASA

NASA Contractor Report 4162

Acousto-Ultrasonic Input-Output Characterization of Unidirectional Fiber Composite Plate by P Waves

Peter Liao and James H. Williams, Jr.
Massachusetts Institute of Technology
Cambridge, Massachusetts

Prepared for
Lewis Research Center
under Grant NAG3-328

National Aeronautics
and Space Administration

**Scientific and Technical
Information Division**

1988

SUMMARY

A unidirectional fiberglass epoxy composite specimen is modelled as a homogeneous transversely isotropic continuum plate-like medium. Acousto-ultrasonic non-contact input-output characterization by tracing the P waves in the continuum is studied theoretically with a transmitting and a receiving transducer located on the same face of the plate. The isotropic plane of the equivalent continuum plate model lies in the midplane of the plate and is parallel to the top and the bottom faces of the plate.

The single reflection problem for an incident P wave at a stress-free plane boundary in a semi-infinite transversely isotropic medium whose isotropic plane is parallel to the plane boundary is analyzed first. It is found that an obliquely incident P wave results in a reflected P wave and a reflected SV wave. One quadrant of each of two sheets of the slowness surfaces of the reflected P and SV waves is plotted. The angle of reflection of the reflected P wave is equal to the angle of incidence of the incident P wave. However, the angle of reflection of the reflected SV wave is smaller than the angle of incident of the incident P wave. Consequently, no critical angle phenomenon occurs. The amplitude ratios of the reflected P and SV waves to the incident P wave as a function of the angle of incidence are plotted. The balance in energy flux normal to the plane boundary is

checked.

The delay time for propagation between the transmitting and the receiving transducers is computed as if the P waves were propagating in an infinite half space. It is found that the directional dependence of the phase velocity of the P waves propagating in the transversely isotropic medium has a significant effect on the delay time, as opposed to the directional independence of the phase velocity of the P waves propagating in an isotropic medium.

The displacements associated with the P waves in the plate and which may be detected by the non-contact receiving transducer are approximated by an asymptotic solution for an infinite transversely isotropic medium subjected to a harmonic point load. The polar diagrams for the directivity functions are plotted at frequencies of 0.75, 1.50 and 2.25 MHz.

The study enhances the quantitative understanding of acousto-ultrasonic nondestructive evaluation (NDE) parameters such as the stress wave factor (SWF) and wave propagation in fiber reinforced composites or any other materials which can be modelled as transversely isotropic media.

INTRODUCTION

Fiber reinforced composite materials are attractive materials for aerospace applications because of their high specific mechanical properties. It has been shown that many composites, such as fiberglass epoxy composites or fiber reinforced ceramics, as shown in Fig. 1, may be modelled as homogeneous transversely isotropic continua [1]. In this work, acousto-ultrasonic (AU) non-contact input-output characterization of a homogeneous transversely isotropic elastic plate is investigated by tracing P waves.

First, the single reflection problem of an incident P wave at a stress-free plane boundary in a semi-infinite transversely isotropic medium, whose isotropic plane is parallel to the plane boundary is considered. At such boundaries, the conditions for the existence of wave mode conversion, the angle of reflection of the reflected wave, and the amplitude ratios of the reflected wave to the incident wave are derived.

Second, the P wave input-output relations are derived when multiple reflections occur at the top and bottom faces of the plate. The delay time between input and output versus the distance separating the transmitting and receiving transducers is analyzed. The directivity functions of the stresses associated with the P waves are computed.

And, the output displacement at the non-contact receiving transducer is approximated by an asymptotic solution.

This investigation should enhance the quantitative understanding of AU NDE parameter such as the stress wave factor. It also provides the potential for assisting in the development of better NDE schemes utilizing the SWF as well as other AU parameters.

SINGLE REFLECTION PROBLEM AT STRESS-FREE PLANE BOUNDARY IN SEMI-INFINITE TRANSVERSELY ISOTROPIC MEDIUM WHOSE ISOTROPIC PLANE IS PARALLEL TO PLANE BOUNDARY FOR INCIDENT P WAVE

1. Reflected P and SV Waves

For a homogeneous linearly elastic transversely isotropic continuum, the number of independent elastic constants is five [1]. Define a coordinate system (x, y, z) for a semi-infinite transversely isotropic medium whose isotropic plane is parallel to the plane boundary where the reflection occurs as follows: the plane boundary contains the x and y axes, and the z axis is the zonal axis of the medium, which is in the direction parallel to the fiber direction shown in Fig. 1. See Fig. 2. The generalized Hooke's law is written, relative to the (x, y, z) coordinate system, as [1]

$$
\begin{aligned}
\tau_{xx} &= C_{11}u,x + C_{12}v,y + C_{13}w,z \\
\tau_{yy} &= C_{12}u,x + C_{11}v,y + C_{13}w,z \\
\tau_{zz} &= C_{13}u,x + C_{13}v,y + C_{33}w,z \\
\tau_{xz} &= C_{44}(u,z + w,x) \\
\tau_{yz} &= C_{44}(v,z + w,y) \\
\tau_{xy} &= C_{66}(u,y + v,x)
\end{aligned}
\qquad (1)
$$

where τ_{rs} (r, s = x, y and z) are the normal (r = s) and shear ($r \neq s$)

stresses with respect to the coordinate system (x, y, z); u, v and w are the displacement components of a point in the medium along the x, y and z axes, respectively; "," denotes partial differentiation with respect to the variable which follows; and C_{11}, C_{12}, C_{13}, C_{33} and C_{44} are the five independent elastic constants where $C_{66} = 1/2(C_{11} - C_{12})$.

Let a plane progressive wave be represented as [2]

$$(u, v, w) = A\,(P_x, P_y, P_z)\,\exp\{i\omega(S_x x + S_y y + S_z z - t)\} \qquad (2)$$

where S_x, S_y and S_z are the components of the slowness vector, which is in the same direction as the normal to the wavefront and whose magnitude is equal to the reciprocal of the magnitude of the phase velocity [1], along the x,y and z axes, respectively; P_x, P_y and P_z are the components of a unit vector of particle displacement along the x, y and z axes, respectively; A is the amplitude of particle displacement; t denotes time and ω denotes radian frequency.

It follows from Eqs. (1) and (2) that the stresses can be represented as

$$\begin{aligned}
\tau_{xx} &= i\omega A[C_{11}S_xP_x + C_{12}S_yP_y + C_{13}S_zP_z]\exp\{i\omega(S_x x + S_y y + S_z z - t)\}\\
\tau_{yy} &= i\omega A[C_{12}S_xP_x + C_{11}S_yP_y + C_{13}S_zP_z]\exp\{i\omega(S_x x + S_y y + S_z z - t)\}\\
\tau_{zz} &= i\omega A[C_{13}S_xP_x + C_{13}S_yP_y + C_{33}S_zP_z]\exp\{i\omega(S_x x + S_y y + S_z z - t)\}\\
\tau_{xz} &= i\omega A[C_{44}S_zP_x + C_{44}S_xP_z]\exp\{i\omega(S_x x + S_y y + S_z z - t)\} \qquad (3)\\
\tau_{yz} &= i\omega A[C_{44}S_zP_y + C_{44}S_yP_z]\exp\{i\omega(S_x x + S_y y + S_z z - t)\}\\
\tau_{xy} &= i\omega A[C_{66}S_yP_x + C_{66}S_xP_y]\exp\{i\omega(S_x x + S_y y + S_z z - t)\}
\end{aligned}$$

The stress boundary conditions on the stress-free plane boundary require that [2]

$$\begin{aligned} \tau_{xz}^{(I)} + \tau_{xz}^{(R)} &= 0 \\ \tau_{yz}^{(I)} + \tau_{yz}^{(R)} &= 0 \\ \tau_{zz}^{(I)} + \tau_{zz}^{(R)} &= 0 \end{aligned} \tag{4}$$

where $\tau_{rz}^{(I)}$ (r=x, y and z) represents stresses on the plane boundary associated with the incident P wave, and $\tau_{rz}^{(R)}$ (r = x, y and z) represents stresses on the plane boundary associated with the reflected waves.

In order to satisfy Eq. (4), it is required that the frequency, ω, of the reflected waves be equal to that of the incident wave and that [2]

$$\begin{aligned} S_x^{(I)} &= S_x^{(R)} \\ S_y^{(I)} &= S_y^{(R)} \quad . \end{aligned} \tag{5}$$

As a result of Eqs. (5), the slowness vectors of the incident and reflected waves lie in a plane called the plane of incidence. This analysis can be simplified by assuming that the plane of incidence is the $x = 0$ plane; that is, the slowness vectors of the incident and reflected waves are in the $x = 0$ plane, as shown in Fig. 2.

Then it follows from Eqs. (5) that

$$S_x^{(I)} = S_x^{(R)} = 0. \tag{6}$$

It has been shown [3] that P waves or SV waves travelling in a plane containing the zonal axis, z axis, of a transversely isotropic medium are quasi-longitudinal and quasi-transverse, respectively; that is, the components of the unit vector of particle displacement for either the P or SV waves along both the y and z axes, P_y and P_z do not vanish; whereas the components along the x axis, P_x, do vanish. Therefore, it follows from Eqs. (3) and (6) that stresses associated with P and SV waves are

$$\begin{aligned} \tau_{xy} &= \tau_{xz} = 0 \\ \tau_{yz} &\neq 0 \; ; \; \tau_{xx} \neq 0 \; ; \; \tau_{yy} \neq 0 \; ; \; \tau_{zz} \neq 0 \; . \end{aligned} \tag{7}$$

It has also been shown that an SH wave travelling in a plane containing the zonal axis, z axis, of a transversely isotropic medium possesses a transverse displacement only; that is, for the coordinates in Fig. 2 $(P_x, P_y, P_z) = (1,0,0)$ [3]. Therefore, it follows from Eqs. (3) and (6) that the stresses associated with SH waves are

$$\begin{aligned} \tau_{xx} &= \tau_{yy} = \tau_{zz} = \tau_{yz} = 0 \\ \tau_{xz} &\neq 0 \; ; \quad \tau_{xy} \neq 0. \end{aligned} \tag{8}$$

Assume that a P wave is incident on the plane boundary. It follows from Eqs. (4) and (7) that

$$\tau_{yz}^{(I)} \neq 0; \quad \tau_{zz}^{(I)} \neq 0$$

$$\tau_{xz}^{(I)} = 0. \tag{9}$$

As a result of Eq.(9), it is immediately known from Eq. (4) that $\tau_{xz}^{(R)}$ is equal to zero. This means that no SH wave will be reflected back into the medium because a reflected wave of the SH type would result in nonzero values of the stress τ_{xz}. So, Eqs. (4) reduce to:

$$\tau_{yz}^{(I)} + \tau_{yz}^{(R)} = 0$$
$$\tau_{zz}^{(I)} + \tau_{zz}^{(R)} = 0. \tag{10}$$

Since either a reflected P wave or a reflected SV wave results in nonzero values of the stresses, $\tau_{yz}^{(R)}$ and $\tau_{zz}^{(R)}$, it is therefore concluded from Eqs. (7) and (10) that both a P wave and an SV wave may be reflected back into the medium.

2. Slowness Surface for P and SV Waves

The equations of motion relative to the coordinate system (x,y,z)

are [1]

$$\begin{aligned} \tau_{xx,x} + \tau_{xy,y} + \tau_{xz,z} &= \rho u,tt \\ \tau_{xy,x} + \tau_{yy,y} + \tau_{yz,z} &= \rho v,tt \\ \tau_{xz,x} + \tau_{yz,y} + \tau_{zz,z} &= \rho w,tt \end{aligned} \tag{11}$$

where the body forces are identically zero for the homogeneous solution.

It follows from Eqs. (1), (2) and (11) that the following equations of motion are obtained:

$$\begin{aligned} &[C_{11}S_x^2 + C_{66}S_y^2 + C_{44}S_z^2 - \rho]P_x + (C_{12} + C_{66})S_xS_yP_y \\ &\quad + (C_{13} + C_{44})S_xS_yP_z = 0 \\ &(C_{12} + C_{66})S_xS_yP_x + [C_{66}S_x^2 + C_{11}S_y^2 + C_{44}S_z^2 - \rho]P_y \\ &\quad + (C_{13} + C_{44})S_yS_zP_z = 0 \\ &(C_{13} + C_{44})S_xS_yP_x + (C_{13} + C_{44})S_yS_zP_y + [C_{44}(S_x^2 + S_y^2) \\ &\quad + C_{33}S_z^2 - \rho]P_z = 0 \end{aligned} \tag{12}$$

The condition for the existence of the plane wave solution is expressed by setting the determinant of the matrix of the coefficients of P_x, P_y and P_z in Eq. (12) equal to zero [1]:

$$\begin{vmatrix} [C_{11}S_x^2 + C_{66}S_y^2 + C_{44}S_z^2 - \rho] & (C_{12} + C_{66})S_xS_y & (C_{13} + C_{44})S_xS_z \\ (C_{12} + C_{66})S_xS_y & [C_{66}S_x^2 + C_{11}S_y^2 + C_{44}S_z^2 - \rho] & (C_{13} + C_{44})S_yS_z \\ (C_{13} + C_{44})S_xS_z & (C_{13} + C_{44})S_yS_z & [C_{44}(S_x^2 + S_y^2) + C_{33}S_z^2 - \rho] \end{vmatrix} = 0 \tag{13}$$

By expanding Eq. (13), three sheets of slowness surface are obtained. The slowness surface for an P wave is given in [3] as

$$\left(\frac{C_{11}+C_{44}}{2}\right)(S_x^2+S_y^2) + \left(\frac{C_{44}+C_{33}}{2}\right)S_z^2 + 1/2\{[(C_{11}-C_{44})(S_x^2+S_y^2) + (C_{33}-C_{44})S_z^2]^2 + 4(S_x^2+S_y^2)S_z^2[(C_{11}-C_{44})(C_{33}-C_{44}) - (C_{13}+C_{44})^2]\}^{1/2} = \rho. \tag{14}$$

Similarly, the slowness surface for an SV wave is given in [3] as

$$\left(\frac{C_{11}+C_{44}}{2}\right)(S_x^2+S_y^2) + \left(\frac{C_{44}+C_{33}}{2}\right)S_z^2 - 1/2\{[(C_{11}-C_{44})(S_x^2+S_y^2) + (C_{33}-C_{44})S_z^2]^2 + 4(S_x^2+S_y^2)S_z^2[(C_{11}-C_{44})(C_{33}-C_{44}) - ((C_{13}+C_{44})^2]\}^{1/2} = \rho. \tag{15}$$

In the present study, the slowness vectors of the incident P wave and the reflected P and SV waves are confined in the y-z plane, as shown in Fig. 2. Take numerical values of elastic constants and density given in [1] for the unidirectional fiberglass epoxy composite as follows: $C_{11} = 10.581 \times 10^9$ N/m^2, $C_{13} = 4.679 \times 10^9$ N/m^2, $C_{33} = 40.741 \times 10^9$ N/m^2, $C_{44} = 4.422 \times 10^9$ N/m^2, and $\rho = 1850$ kg/m^3. One quadrant of the intersection of the slowness surface of a P wave travelling in the unidirectional fiberglass epoxy composite with the plane x = 0 and one quadrant of the intersection of the slowness surface of an SV wave travelling in the unidirectional fiberglass epoxy composite with the plane x = 0 are obtained by substituting the numerical values of the elastic constants and the density given above into Eqs. (14) and (15), respectively, and are shown in Fig. 3.

3. Angle of Reflection

It follows from Eqs. (5) and (6) that the y-component of the slowness vector of an incident P wave is equal to the y-component of the reflected P wave as well as the y-component of the reflected SV wave. Accordingly, the relation between the y-component of the slowness vector of an incident P wave and the y-components of the slowness vectors of the reflected P and SV waves is given as

$$S_y^{(I)} = S_y^{(P)} = S_y^{(SV)} = b \tag{16}$$

where $S_y^{(I)}$ represents the y-component of the slowness vector of an incident P wave; $S_y^{(P)}$ represents the y-component of the slowness vectors of the reflected P wave; $S_y^{(SV)}$ represents the y-component of the slowness vector of the reflected SV waves; and b is a common constant.

It follows from Eqs. (6), (14) and (16) that the relation between the z-component of the slowness vector of an incident P wave and that of the reflected P wave is

$$S_z^{(I)} = -S_z^{(P)} \tag{17}$$

The minus sign is due to the fact that the slowness vector of an incident P wave points out of the medium, whereas the slowness vector of the reflected P wave points into the medium, as shown in Fig. 2. Consequently, the value of the z-component of the slowness vector of an incident P wave, $S_z^{(I)}$, is negative, whereas that of the reflected P wave, $S_z^{(P)}$, is positive.

The angle of reflection is defined as the angle between the slowness vector of a reflected wave, either type P or SV, and the normal to the plane boundary where the reflection occurs. Similarly, the angle of incidence is defined as the angle between the slowness vector of an incident P wave and the normal to the plane boundary, as

shown in Fig. 2. Therefore, the angle of reflection of a reflected P wave θ_p is

$$\theta_p = \tan^{-1}(S_y^{(P)}/S_z^{(P)}) \tag{18}$$

and the angle of incidence of an incident P wave θ_I is

$$\theta_I = \tan^{-1}(S_y^{(I)}/-S_z^{(I)}). \tag{19}$$

It follows from Eqs. (16), (17), (18) and (19) that the angle of incidence of an incident P wave is equal to the angle of reflection of the reflected P wave, as shown in Fig. 2.

However, the angle of reflection of the reflected SV wave is not equal to the angle of incidence of the incident P wave. For a given value of b in Eq. (16), two values of the z-component of the slowness vector, S_z, of equal magnitude but opposite sign of an SV wave travelling in the plane x = 0 in the transversely isotropic medium can be obtained from the slowness surface for the SV wave from Eqs. (6) and (15). The positive z-component of the slowness vector corresponds to the reflected SV wave and is denoted as $S_z^{(SV)}$. Similarly, for a given value of b, there exists a positive z-component of the slowness vector, $S_z^{(P)}$, corresponding to the reflected P wave. Accordingly, for any given value of b in Eq. (16), there exist a positive z-compo-

nent of the slowness vector for the reflected P wave, $S_z^{(P)}$, and a positive z-component of the slowness vector for the reflected SV wave, $S_z^{(SV)}$. In fact, the z-components of the slowness vectors of the reflected P and SV waves, $S_z^{(P)}$ and $S_z^{(SV)}$, for an incident P wave which determines the value of b in Eq. (16) and which travels in the plane x = 0 in the transversely isotropic medium, can be obtained from the lengths of the perpendicular lines between the abscissa representing the value of b and the interesections with two sheets of slowness surface for the reflected P wave and the reflected SV wave, respectively, as shown in Fig. 3. It is apparent from Fig. 3 that the z-component of the slowness vector of the reflected P wave, $S_z^{(P)}$, is less than that of the reflected SV wave, $S_z^{(SV)}$, for an incident P wave travelling in the plane x = 0 in the unidirectional fiberglass epoxy composite under consideration [1]. Consequently, the angle of reflection of the reflected SV wave θ_{SV} defined similarly to Eq. (18) as

$$\theta_{SV} = \tan^{-1} (S_y^{(SV)}/S_z^{(SV)}), \tag{20}$$

is smaller than the angle of reflection of the reflected P wave, from Eqs. (16), (18) and (20). The angle of reflection of the reflected SV wave as a function of the angle of incidence of an incident P wave travelling in the unidirectional fiberglass epoxy composite [1] is shown in Fig. 4.

The critical angle is defined as the angle of incidence of an incident P wave at which the slowness vector of the reflected SV wave (or P wave) becomes tangent to the plane boundary where the reflection occurs. For the case of an incident P wave travelling in the unidirectional fiberglass epoxy composite in Fig. 1, it has been shown that the angle of reflection of the reflected SV wave is smaller than that of the reflected P wave. Thus, the critical angle phenomenon does not occur for the unidirectional fiberglass epoxy composite under consideration. This is due to the fact that when the angle of incidence of an incident P wave reaches 90^{o}, the angle of reflection of the reflected SV wave is still less than 90^{o}.

4. Amplitude Ratios of Reflected Waves to Incident Wave

It has been shown that when a P wave travelling in a semi-infinite transversely isotropic medium is incident on a plane boundary, a P wave and an SV wave will be reflected. The boundary conditions on the stresses of a P wave travelling in the plane $x = 0$ and incident on the plane boundary can be obtained from Eqs. (4) and (7) as

$$\tau_{yz}^{(I)} + \tau_{yz}^{(SV)} + \tau_{yz}^{(P)} = 0 \qquad (21)$$

$$\tau_{zz}^{(I)} + \tau_{zz}^{(SV)} + \tau_{zz}^{(P)} = 0$$

where $\tau_{yz}^{(I)}$ and $\tau_{zz}^{(I)}$ represent the shear and normal stresses associated with the incident P wave; $\tau_{yz}^{(SV)}$ and $\tau_{zz}^{(SV)}$ represent the shear and normal stresses associated with the reflected SV wave; and $\tau_{yz}^{(P)}$ and $\tau_{zz}^{(P)}$ represents the shear and normal stresses associated with the reflected P wave.

The shear stress, $\tau_{yz}^{(I)}$, associated with a P wave of unit amplitude travelling in the plane $x = 0$ and incident on the plane boundary at the origin, as shown in Fig. 2, can be obtained from Eqs. (3) and (6) as

$$\tau_{yz}^{(I)} = i\omega(C_{55}S_z^{(I)}P_y^{(I)} + C_{55}S_y^{(I)}P_z^{(I)}) \tag{22}$$

where $S_y^{(I)}$ and $S_z^{(I)}$ are the components of the slowness vector of the incident P wave along the y and z axes, respectively; $P_y^{(I)}$ and $P_z^{(I)}$ are the components of the unit vector of particle displacement of the incident P wave along the y and z axes, respectively; C_{55} is an elastic constant; and ω is the frequency. Similarly, the normal stress, $\tau_{zz}^{(I)}$, associated with the incident P wave of unit amplitude can be expressed, from Eqs. (3) and (6), as

$$\tau_{zz}^{(I)} = i\omega(C_{13}S_y^{(I)}P_y^{(I)} + C_{33}S_z^{(I)}P_z^{(I)}) \tag{23}$$

where C_{13} and C_{33} are elastic constants.

The shear stress, $\tau_{yz}^{(P)}$, and the normal stress, $\tau_{zz}^{(P)}$, associated with the reflected P wave on the plane boundary at the origin are, from Eqs. (3) and (6),

$$\tau_{yz}^{(P)} = i\omega A^{(P)}(C_{55}S_z^{(P)}P_y^{(P)} + C_{55}S_y^{(P)}P_z^{(P)}) \tag{24}$$

and

$$\tau_{zz}^{(P)} = i\omega A^{(P)}(C_{13}S_y^{(P)}P_y^{(P)} + C_{33}S_z^{(P)}P_z^{(P)}). \tag{25}$$

where $S_y^{(P)}$ and $S_z^{(P)}$ are the components of the slowness vector of the reflected P wave along the y and z axes, respectively; $P_y^{(P)}$ and $P_z^{(P)}$ are the components of the unit vector of particle displacement of the reflected P wave along the y and z axes, respectively; and $A^{(P)}$ is the amplitude of the reflected P wave.

The shear stress, $\tau_{yz}^{(SV)}$, and the normal stress, $\tau_{zz}^{(SV)}$, associated with the reflected SV wave on the plane boundary at the origin, from Eqs. (3) and (6),

$$\tau_{yz}^{(SV)} = i\omega A^{(SV)}(C_{55}S_z^{(SV)}P_y^{(SV)} + C_{55}S_y^{(SV)}P_z^{(SV)}) \tag{26}$$

and

$$\tau_{zz}^{(SV)} = i\omega A^{(SV)}(C_{13}S_y^{(SV)}P_y^{(SV)} + C_{33}S_z^{(SV)}P_z^{(SV)}). \tag{27}$$

where $S_y^{(SV)}$ and $S_z^{(SV)}$ are the components of the slowness vector of

the reflected SV wave along the y and z axes, respectively; $P_y^{(SV)}$ and $P_z^{(SV)}$ are the components of the unit vector of particle displacement of the reflected SV wave along the y and z axes, respectively; and $A^{(SV)}$ is the amplitude of the reflected SV wave.

Upon substitution of Eqs. (22) through (27) into Eq. (21), the boundary conditions on the stresses for an incident P wave of unit amplitude travelling in the plane x = 0 can be rewritten as

$$S_z^{(I)}P_y^{(I)} + S_y^{(I)}P_z^{(I)} + A^{(P)}(S_z^{(P)}P_y^{(P)} + S_y^{(P)}P_z^{(P)}) + A^{(SV)}(S_z^{(SV)}P_y^{(SV)} + S_y^{(SV)}P_z^{(SV)}) = 0$$

$$(C_{13}S_y^{(I)}P_y^{(I)} + C_{33}S_z^{(I)}P_z^{(I)}) + A^{(P)}(C_{13}S_y^{(P)}P_y^{(P)} + C_{33}S_z^{(P)}P_z^{(P)}) + A^{(SV)}(C_{13}S_y^{(SV)}P_y^{(SV)} + C_{33}S_z^{(SV)}P_z^{(SV)}) = 0 \qquad (28)$$

The components of a unit vector of particle displacement along the y and z axes of a P wave travelling in any plane containing the zonal axis of a transversely isotropic medium are given in [3], and can be expressed, when applied to the present case of the reflected P wave travelling in the plane x = 0, as [3]

$$P_y(P) = [H_p - (C_{33}-C_{44})S_z(P)^2]/$$
$$\{[H_p-(C_{33}-C_{44})S_z(P)^2]^2$$
$$+ [(C_{13}+C_{44})S_y(P)S_z(P)]^2\}^{1/2}$$
$$P_z(P) = (C_{13}+C_{44})S_y(P)S_z(P)/ \tag{29}$$
$$\{[H_p-(C_{33}-C_{44})S_z(P)^2]^2$$
$$+ [(C_{13}+C_{44})S_y(P)S_z(P)]^2\}^{1/2}$$

where C_{13}, C_{33} and C_{44} are elastic constants; and H_p is defined as

$$H_p = \{(C_{11}-C_{44})S_y(P)^2 + (C_{33}-C_{44})S_z(P)^2$$
$$+ \{[(C_{11}-C_{44})S_y(P)^2$$
$$+ (C_{33}-C_{44})S_z(P)^2]^2$$
$$- 4S_y(P)^2S_z(P)^2[(C_{11}-C_{44})(C_{33}-C_{44})$$
$$- (C_{13}+C_{44})^2]^2\}^{1/2}\}/2.$$

Similarly, the components of a unit vector of particle displacement along the y and z axes for the reflected SV waves travelling in the plane x = 0 can be expressed as

$$P_y^{(SV)} = [H_{SV} - (C_{33}-C_{44})S_z^{(SV)2}]/$$

$$\{[H_{SV} - (C_{33}-C_{44})S_z^{(SV)2}]^2$$

$$+ [(C_{13}+C_{44})S_y^{(SV)}S_z^{(SV)}]^2\}^{1/2} \qquad (30)$$

$$P_z^{(SV)} = (C_{13}+C_{44})S_y^{(SV)}S_z^{(SV)}/$$

$$\{[H_{SV} - (C_{33}-C_{44})S_z^{(SV)2}]^2$$

$$+ [(C_{13}+C_{44})S_y^{(SV)}S_z^{(SV)}]^2\}^{1/2}$$

where H_{SV} is defined as

$$H_{SV} = \{(C_{11}-C_{44})S_y^{(SV)2} + (C_{33}-C_{44})S_z^{(SV)2}$$

$$- \{[(C_{11}-C_{44})S_y^{(SV)2} + (C_{33}-C_{44})S_z^{(SV)2}]^2$$

$$- 4S_y^{(SV)2}\,S_z^{(SV)2}\,[(C_{11}-C_{44})(C_{33}-C_{44})$$

$$- (C_{13}+C_{44})^2]^2\}^{1/2}\}/2.$$

The amplitude ratios of the reflected P and SV waves, $A^{(P)}$ and $A^{(SV)}$, for a P wave of unit amplitude obliquely incident on the plane boundary can be determined from Eq. (28). For a given incident P wave, the values of the components of the slowness vector along the y and z axes, $S_y^{(I)}$ and $S_z^{(I)}$, and the values of the components of the unit vector of particle displacement along the y and z axes, $P_y^{(I)}$ and

$P_z^{(I)}$, are defined as part of the the specification of the incident P wave. The values of the components of the slowness vector of the reflected P wave along the y and z axes, $S_y^{(P)}$ and $S_z^{(P)}$, are determined from Eqs. (16) and (17), respectively. The values of the components of the unit vector of particle displacement along the y and z axes for the reflected P wave, $P_y^{(P)}$ and $P_z^{(P)}$, are obtained by substituting $S_y^{(P)}$ and $S_z^{(P)}$ into Eq. (29). The values of the coefficients for $A^{(P)}$ in Eq. (28) are thus obtained. Since the y-component of the slowness vector of the reflected SV wave, $S_y^{(SV)}$, is equal to that of the incident P wave, Eq. (16), the value of the z-component of the reflected SV wave, $S_z^{(SV)}$, is obtained by substituting $S_y^{(I)}$ into the slowness surface for the SV wave, Eq. (15). On substitution of the values of the $S_z^{(SV)}$ and $S_y^{(SV)}$ into Eq. (30), the values of the unit vector of particle displacement along the y and z axes for the reflected SV wave, $P_y^{(SV)}$ and $P_z^{(SV)}$, are determined. The values of the coefficients for $A^{(SV)}$ in Eq. (28) are thus obtained. The values of the amplitudes of the reflected P and SV waves, $A^{(P)}$ and $A^{(SV)}$, are then obtained by solving Eq. (28) with the thus determined values of the coefficients for $A^{(P)}$ and $A^{(SV)}$ in Eq. (28) for a given incident P wave. By varying the angle of incidence of the incident P wave of unit amplitude and by repeating the procedures described above, the amplitude ratios of the reflected P and SV waves to the incident P wave are obtained as functions of the angle of incidence. For an incident P wave in the unidirectional fiberglass

epoxy composite shown in Fig. 1, the amplitude ratios of the reflected P and SV waves to the incident P wave versus the angle of incidence are shown in Fig. 5.

5. Balance in Energy Flux Normal to Plane Boundary

The balance in energy flux normal to the plane boundary $z = 0$, as shown in Fig. 2, must be satisfied and is expressed as [2]

$$F_z^{(I)} + F_z^{(P)} + F_z^{(SV)} = 0 \tag{31}$$

where $F_z^{(I)}$, $F_z^{(P)}$ and $F_z^{(SV)}$ are the z-components of the energy fluxes of the incident P wave, the reflected P wave and the reflected SV wave, respectively.

The z-component of the energy flux of an incident P wave of unit amplitude travelling in the plane $x = 0$ is [4]

$$F_z^{(I)} = \omega^2(C_{44}P_y^{(I)2}\, S_z^{(I)} + C_{13}P_y^{(I)}P_z^{(I)}S_y^{(I)} + C_{44}P_y^{(I)}P_z^{(I)}S_y^{(I)} + C_{33}P_z^{(I)2}S_z^{(I)}) \tag{32}$$

where $P_y^{(I)}$ and $P_z^{(I)}$ are the components of the unit vector of particle displacement of the incident P wave along the y and z axes,

respectively; $S_y^{(I)}$ and $S_z^{(I)}$ are the components of the slowness vector of the incident P wave along the y and z axes, respectively; ω is the radian frequency; and C_{13}, C_{33} and C_{44} are elastic constants.

Similarly, the z-components of the energy fluxes of the reflected P wave and the reflected SV wave are [4]

$$F_z^{(P)} = A^{(P)^2}\,\omega^2(C_{44}P_y^{(P)^2}\,S_z^{(P)} + C_{13}P_y^{(P)}P_z^{(P)}S_y^{(P)} + C_{44}P_y^{(P)}P_z^{(P)}S_y^{(P)} + C_{33}P_z^{(P)^2}S_z^{(P)}) \tag{33}$$

and

$$F_z^{(SV)} = A^{(SV)^2}\omega^2(C_{44}P_y^{(SV)^2}S_z^{(SV)} + C_{13}P_y^{(SV)}P_z^{(SV)}S_y^{(SV)} + C_{44}P_y^{(SV)}P_z^{(SV)}S_y^{(SV)} + C_{33}P_z^{(SV)^2}S_z^{(SV)}) \tag{34}$$

Since the frequency term ω^2 is common to Eqs. (32), (33) and (34), the balance in energy flux normal to the plane boundary, Eq. (31), is not affected by assuming the value of the frequency ω to be equal to unity. Accordingly, subsequent calculations of the values of the z-components of the energy fluxes of the incident P wave and the reflected P and SV waves, $F_z^{(I)}$, $F_z^{(P)}$ and $F_z^{(SV)}$, are done by assuming the radian frequency ω to be equal to one.

The values of the z-components of the energy fluxes in Eqs. (32), (33) and (34) are obtained similarly to the calculations of the amplitude ratios of the reflected P and SV waves to the incident P wave. For a given incident P wave of unit amplitude, the y-components of the slowness vectors and of the unit vectors of particle displacement, $S_y^{(I)}$, $S_y^{(P)}$, $S_y^{(SV)}$, $P_y^{(I)}$, $P_y^{(P)}$ and $P_y^{(SV)}$, and the z-components of the slowness vectors and of the unit vectors of particle displacement, $S_z^{(I)}$, $S_z^{(P)}$, $S_z^{(SV)}$, $P_z^{(I)}$, $P_z^{(P)}$ and $P_z^{(SV)}$ of the incident P wave and of the reflected P and SV waves are determined first. Then, combining the amplitudes of the reflected P and SV waves, $A^{(P)}$ and $A^{(SV)}$, with the values of $S_y^{(I)}$, $S_y^{(P)}$, $S_y^{(SV)}$, $S_z^{(I)}$, $S_z^{(P)}$, $S_z^{(SV)}$, $P_y^{(I)}$, $P_y^{(P)}$, $P_y^{(SV)}$, $P_z^{(I)}$, $P_z^{(P)}$ and $P_z^{(SV)}$, the values of the z-components of the energy fluxes of the incident P wave and the reflected P and SV waves, $F_z^{(I)}$, $F_z^{(P)}$ and $F_z^{(SV)}$, are thus obtained from Eqs. (32), (33) and (34). For a P wave of unit amplitude travelling in the plane $x = 0$ in the unidirectional fiberglass epoxy composite shown in Fig. 1 incident on a plane boundary, the z-components of the energy fluxes of the reflected P and SV waves and the energy flux of the incident P wave are shown in Fig. 6 with the value of the frequency ω in Eqs. (32), (33) and (34) equal to one. The balance in energy flux normal to the plane boundary, Eq. (31), is also checked and is shown in Fig. 6.

ACOUSTO-ULTRASONIC NON-CONTACT INPUT-OUTPUT CHARACTERIZATION OF UNIDIRECTIONAL FIBERGLASS EPOXY COMPOSITE PLATE

It has been shown [1] that the unidirectional fiber composite shown in Fig. 1 may be modelled as a homogeneous transversely isotropic continuum. For the axes shown in Fig. 1, the isotropic plane of its equivalent continuum lie in the midplane of the plate [1]. A cartesian coordinate system (x, y, z) is chosen so that the x-y plane is the isotropic plane; as a result, the upper and the lower surface are at $z = h/2$ and $z = -h/2$, respectively, where h is the plate thickness. The properties of the equivalent continuum model of the unidirectional fiberglass epoxy composite plate to be considered are [1]

$$
\begin{aligned}
h &= 0.1 \text{ m} \\
C_{11} &= 10.581 \times 10^9 \text{ N/m}^2 \\
C_{13} &= 4.679 \times 10^9 \text{ N/m}^2 \\
C_{33} &= 40.741 \times 10^9 \text{ N/m}^2 \\
C_{44} &= 4.422 \times 10^9 \text{ N/m}^2 \\
C_{66} &= 3.243 \times 10^9 \text{ N/m}^2 \\
\rho &= 1850 \text{ kg/m}^3
\end{aligned}
\tag{35}
$$

A transmitting and a receiving transducer are located on the same face of the unidirectional fiberglass epoxy composite plate specimen without direct contact, as shown in Fig. 7. The unidirectional

fiberglass epoxy composite plate specimen shown in Fig. 7 is considered as a plate of thickness h and of infinite planar (x-y) extent. The input electrical voltage to the transmitting transducer is $V_i(t)$ and the output electrical voltage from the receiving transducer is $V_o(t)$ where t represents time. The transmitting transducer converts an input electrical voltage into a stress, whereas the receiving transducer converts a displacement associated with stress waves travelling in the plate into an output voltage. In the following analysis, only the P waves are traced. The P waves which are generated by the transmitting transducer located above point O experience multiple reflections at each face of the plate, and then reach the receiving transducer located above point M, as shown in Fig. 8. Since the isotropic plane lies in the midplane and is parallel to both the top and the bottom faces where the multiple reflections occur, the angle of reflection of the reflected P wave is equal to the angle of incidence of an incident P wave for each reflection at each face of the plate. Accordingly, the P wave travelling from the input O to the output M may be considered as a wave propagating in a semi-infinite transversely isotropic medium, and travelling to point M' as if there were no bottom face, as shown in Fig. 8.

1. Delay Time and Phase Velocity

Let the input O and the output M lie in the y-z plane. Assume

the number of reflections at the bottom face experienced by the P wave in travelling from the input O to the output M is n, as shown in Fig. 8. With respect to the z axis, the angle of incidence of the P wave at each face of the plate is θ, and the total distance travelled by the wave is R_n. From the geometry in Fig. 8,

$$\theta = \tan^{-1}(\ell/2nh) \tag{36}$$

where ℓ is the separation distance between the input O and the output M, and

$$R_n = \ell/\sin\theta \tag{37}$$

The time delay t_n for the wave to reach the receiving transducer is

$$t_n = R_n/C_1(\theta) \tag{38}$$

where $C_1(\theta)$ is the directionally dependent phase velocity of the P wave. The phase velocity C_1 of a P wave in the unidirectional fiber-glass epoxy composite shown in Fig. 1 is given as [1]

$$C_1(\theta) = [(C_{44}+C_{11}\sin^2\theta + C_{33}\cos^2\theta + \sqrt{E})/2\rho]^{1/2} \tag{39}$$

where

$$E = [(C_{11}-C_{44})\sin^2\theta + (C_{44}-C_{33})\cos^2\theta]^2 + 4(C_{13}+C_{44})^2\sin^2\theta\cos^2\theta ;$$

C_{11}, C_{13}, C_{33}, C_{44} and ρ are given by Eq. (35).

The delay time is then computed when the number of reflections n at the bottom face of the plate is equal to 10, 100, 300 or 500. The numerical results are shown in Fig. 9 where the delay time t_n is plotted as the ordinate, and the dimensionless separation ℓ/h is plotted as the abscissa, for values of zero to 300. The phase velocity C_1 as a function of the angle of incidence θ is also shown in Fig. 10.

2. Displacements Detected by Receiving Transducer

The displacements detected by the non-contact receiving transducer above point M, radiated by the non-contact transmitting transducer, are assumed to be equivalent to the displacements at point M' associated with the P wave propagating in a semi-infinite transversely isotropic medium as if there were no bottom boundary (except for the cumulative effect of the reflection coefficient), as shown in Fig. 8. The displacements at point M' are approximated by the far-field asymptotic solution for large R_n of an infinite transversely isotropic medium subjected to a harmonic point load.

Consider an infinite transversely isotropic medium in which the z axis of a rectangular cartesian system 0(x, y, z) is the zonal axis

of the medium and the x-y plane coincides with the isotropic plane, as shown in Fig. 11. The equations of motion including the body forces are [5]

$$\tau_{xx,x} + \tau_{xy,y} + \tau_{xz,z} + \rho X = \rho u,tt \tag{40}$$

$$\tau_{xy,x} + \tau_{yy,y} + \tau_{yz,z} + \rho Y = \rho v,tt \tag{41}$$

$$\tau_{xz,x} + \tau_{yz,y} + \tau_{zz,z} + \rho Z = \rho w,tt \tag{42}$$

where τ_{rs} (r, s = x, y and z) are the normal (r = s) and shear ($r \neq s$) stresses with respect to the chosen coordinate system O(x, y, z); u, v and w are displacement components of a point in the medium along the x, y and z axes, respectively; X, Y and Z are the components of the body force along the x, y and z axes respectively; ρ is the density; t is time; and "," denotes partial differentiation with respect to the variable which follows.

Combining Eqs. (1)and (42) gives

$$\Gamma,_{tt} = \left(\frac{C_{13}+C_{44}}{\rho}\right) \Delta,_{zz} + \frac{C_{44}}{\rho} \Gamma,_{xx} + \frac{C_{44}}{\rho} \Gamma,_{yy} + \frac{C_{33}}{\rho} \Gamma,_{zz} + Z,_{z} \tag{43}$$

where Γ and Δ are given by [5].

$$\Gamma = w,z; \quad \Delta = u,x + v,y.$$

By differentiating Eq. (40) with respect to x and Eq. (41) with respect to y, we find upon addition of the resulting equations and using the appropriate stress-strain relations, Eq. (1), that

$$\Delta,tt = \left(\frac{C_{13}+C_{44}}{\rho}\right)(\Gamma,xx + \Gamma,yy) + \frac{C_{44}}{\rho}\Delta,zz$$

$$+\frac{C_{11}}{\rho}(\Delta,xx + \Delta,yy) + X,x + Y,y \tag{44}$$

For a harmonic point load at the origin, the body forces may be taken of the form [5]

$$\begin{aligned} X &= X_o\delta(x)\delta(y)\delta(z)e^{-i\omega t} \\ Y &= Y_o\delta(x)\delta(y)\delta(z)e^{-i\omega t} \\ Z &= Z_o\delta(x)\delta(y)\delta(z)e^{-i\omega t} \end{aligned} \tag{45}$$

where $\delta(r)$ ($r = x$, y and z) is the Dirac delta function; and X_o, Y_o and Z_o are the magnitudes of the respective point body forces. Express Γ and Δ as threefold Fourier integrals [5] as follows.

$$\Gamma(x,y,z,t) = \int_{-\infty}^{\infty}\int\int\int \bar{\Gamma}\ (S_x,S_y,S_z,t)$$

$$\exp\{i\omega(S_x x+S_y y+S_z z-t)\}dS_x dS_y dS_z \qquad (46)$$

$$\Delta(x,y,z,t) = \int_{-\infty}^{\infty}\int\int\int \bar{\Delta}(S_x,S_y,S_z,t)$$

$$\exp\{i\omega(S_x x+S_y y+S_z z-t)\}dS_x dS_y dS_z$$

where

$$\bar{\Gamma}(S_x,S_y,S_z,t) = 1/8\pi^3 \int_{-\infty}^{\infty}\int\int\int \Gamma(x,y,z,t)$$

$$\exp\{i\omega(-S_x x-S_y y-S_z z+ t)\}dxdydz.$$

$$\bar{\Delta}(S_x,S_y,S_z,t) = 1/8\pi^3 \int_{-\infty}^{\infty}\int\int\int \Delta(x,y,z,t)$$

$$\exp\{i\omega(-S_x x-S_y y-S_z z+ t)\}dxdydz.$$

Similarly, X,x, Y,y and Z,z can be expressed as threefold

Fourier integrals [5]

$$X,x = i\omega S_x \iiint_{-\infty}^{\infty} \bar{X} \exp\{i\omega(S_x x + S_y y + S_z z - t)\} dS_x dS_y dS_z \qquad (47)$$

$$Y,y = i\omega S_y \iiint_{-\infty}^{\infty} \bar{Y} \exp\{i\omega(S_x x + S_y y + S_z z - t)\} dS_x dS_y dS_z \qquad (48)$$

$$Z,z = i\omega S_z \iiint_{-\infty}^{\infty} \bar{Z} \exp\{i\omega(S_x x + S_y y + S_z z - t)\} dS_x dS_y dS_z \qquad (49)$$

where

$$\bar{X} = 1/8\pi^3 \iiint_{-\infty}^{\infty} X_o \delta(x)\delta(y)\delta(z) e^{-i\omega t}$$

$$\exp\{i\omega(-S_x x - S_y y - S_z z + t\} dS_x dS_y dS_z$$

$$= X_o/8\pi^3$$

and, similarly,

$$\bar{Y} = \frac{Y_o}{8\pi^3} \; ; \quad \bar{Z} = \frac{Z_o}{8\pi^3} \; .$$

Substitution of Eqs. (45) through (49) into Eqs. (43) and (44)

gives

$$\bar{\Delta} = \frac{C_{44}/\rho\ (S_x^2+S_y^2) + C_{33}/\rho\ S_z^2-1}{8\pi^3\ \omega H\ (S_x,\ S_y,\ S_z)}\ (iS_xX_o + iS_yY_o) +$$

$$\frac{-(C_{13}+C_{44})/\rho\ (S_x^2+S_y^2)}{8\pi^3\ \omega H\ (S_x,\ S_y,\ S_z)}\ iS_zZ_o \qquad (50)$$

$$\bar{\Gamma} = \frac{-(C_{13}+C_{44})/\rho\ S_z^2}{8\pi^3\ \omega H\ (S_x,\ S_y,\ S_z)}\ (iS_xX_o + iS_yY_o) +$$

$$\frac{C_{11}/\rho\ (S_x^2 + S_y^2) + C_{33}/\rho\ S_z^2 - 1}{8\pi^3\ \omega H\ (S_x,\ S_y,\ S_z)}\ iS_zZ_o \qquad (51)$$

where

$$H(S_x,S_y,S_z) = \left[\frac{C_{44}}{\rho}\ S_z^2 + \frac{C_{11}}{\rho}\ (S_x^2+S_y^2) - 1\right]$$

$$\left[\frac{C_{44}}{\rho}\ (S_x^2+S_y^2) + \frac{C_{33}}{\rho}\ S_z^2 - 1\right]$$

$$- \left(\frac{C_{44}+C_{13}}{\rho}\right)^2\ S_z^2\ (S_x^2+S_y^2). \qquad (52)$$

In fact, $H(S_x,\ S_y,\ S_z) = 0$ represents two sheets of the slowness surface, one for a P wave and one for an SV wave [5]. As a result of Eqs. (50) and (51), Γ and Δ in Eq. (46) can be written as

$$\Gamma(x,y,z,t) = \iiint_{-\infty}^{\infty} \left[\frac{-(C_{13}+C_{44})/\rho \; S_z^2}{8\pi^3\omega H(S_x,S_y,S_z)} (iS_xX_o+iS_yY_o) \right.$$

$$\left. + \frac{C_{11}/\rho \; (S_x^2+S_y^2) + C_{33}/\rho \; S_z^2 - 1}{8\pi^3\omega H(S_x,S_y,S_z)} iS_zZ_o \right]$$

$$\exp\{i\omega(S_xx+S_yy+S_zz-t)\}dS_xdS_ydS_z \qquad (53)$$

$$\Delta(x,y,z,t) = \iiint_{-\infty}^{\infty} \left[\frac{C_{44}/\rho \; (S_x^2+S_y^2) + C_{33}/\rho \; S_z^2 - 1}{8\pi^3\omega H(S_x,S_y,S_z)} (iS_xX_o+iS_yY_o) \right.$$

$$\left. + \frac{-(C_{13}+C_{44})/\rho \; (S_x^2+S_y^2)}{8\pi^3\omega H(S_x,S_y,S_z)} iS_zZ_o \right]$$

$$\exp\{i\omega(S_xx + S_yy + S_zz - t)\}dS_xdS_ydS_z \qquad (54)$$

The asymptotic solution at a large distance from the point load is obtained by applying the theory of residues, the method of stationary phase, and the radiation condition [5] as

$$\Gamma(x,y,z,t) \sim \frac{\lambda_n\omega}{2\pi R} \left[\frac{-(C_{13}+C_{44})}{\rho} S_z^{*2}(iS_x^* X_o+iS_y^* Y_o) \right.$$

$$\left. + \left(\frac{C_{11}}{\rho} (S_x^{*2}+ S_y^{*2}) + \frac{C_{33}}{\rho} S_z^{*2} - 1\right)iS_z^* Z_o \right]$$

$$\exp\{i\omega(S_x^*x + S_y^*y + S_z^*z - t)\} \qquad (55)$$

$$\Delta(x,y,z,t) \sim \frac{\lambda_n\omega}{2\pi R} \left\{ \left[\frac{C_{44}}{\rho}(S_x^{*2}+ S_y^{*2}) + \frac{C_{33}}{\rho} S_z^{*2} - 1\right](iS_x^* X_o+iS_y^* Y_o) \right.$$

$$\left. + \frac{-(C_{13}+C_{44})}{\rho} (S_x^{*2}+ S_y^{*2}) iS_z^* Z_o \right\}$$

$$\exp\{i\omega(S_x^*x + S_y^*y + S_z^*z - t)\} \qquad (56)$$

where R is the distance from the origin 0 where the point loads are applied to the location of interest Q in the medium, as shown in Fig. 11; (S_x^*, S_y^*, S_z^*) are points on the slowness surface for a P wave where the normal is parallel to the OQ direction; λ_n is the amplitude coefficient and is given by

$$\lambda_n = \left\{ \frac{H_{,Sx}^2 + H_{,Sy}^2}{\Sigma[H_{,Sz}^2(H_{,SxSx}\, H_{,SySy} - H_{,SxSy}^2) + H_{,Sz}^2}{2H_{,Sx}H_{,Sy}(H_{,SxSz}H_{,SySz} - H_{,SxSy}H_{,SzSz})]} \right\}^{1/2} \tag{57}$$

where Σ is the sum with respect to cyclic permutation of S_x, S_y and S_z, and is evaluated at points (S_x^*, S_y^*, S_z^*) on the slowness for a P wave where the normal is parallel to the OQ direction.

The displacement components along the x, y and z axes, u, v and w, due to a P wave can be obtained by direct integration of the definitions of Γ and Δ in Eq. (43), and are given as [6]

$$\begin{aligned} u &= \frac{S_x}{i\omega(S_x^2+S_y^2)}\,\Delta \\ v &= \frac{S_y}{i\omega(S_x^2+S_y^2)}\,\Delta \\ w &= \frac{1}{i\omega S_z}\,\Gamma \end{aligned} \tag{58}$$

Substitution of Eqs. (55) and (56) into Eq. (58) gives the asymptotic solutions at a large distance of the displacement components along the x, y and z axes, u, v and w, as follows:

$$u \sim \frac{-i\lambda_n S_x^*}{2\pi R(S_x^{*2}+ S_y^{*2})} \left\{ \left[\frac{C_{44}}{\rho} (S_x^{*2}+ S_y^{*2}) + \frac{C_{33}}{\rho} S_z^{*2} - 1\right](iS_x^* X_o + iS_y^* Y_o) \right.$$

$$\left. + \frac{-(C_{13}+C_{44})}{\rho} (S_x^{*2} + S_y^{*2})\, iS_z^* Z_o \right\}$$

$$\exp\{i\omega(S_x^* x + S_y^* y + S_z^* z - t)\} \qquad (59)$$

$$v \sim \frac{-i\lambda_n S_y^*}{2\pi R(S_x^{*2}+ S_y^{*2})} \left\{ \left[\frac{C_{44}}{\rho} (S_x^{*2} + S_y^{*2}) + \frac{C_{33}}{\rho} S_z^{*2} - 1\right](iS_x^* X_o + iS_y^* Y_o) \right.$$

$$\left. + \frac{-(C_{13}+C_{44})}{\rho} (S_x^{*2}+ S_y^{*2}) iS_z^* Z_o \right\}$$

$$\exp\{i\omega(S_x^* x + S_y^* y + S_z^* z - t)\} \qquad (60)$$

$$w \sim \frac{\lambda_n}{2\pi R} \left[\frac{-(C_{13} + C_{44})}{\rho} S_z^* (S_x^* X_o + S_y^* Y_o) \right.$$

$$\left. + \left(\frac{C_{11}}{\rho} (S_x^{*2}+ S_y^{*2}) + \frac{C_{33}}{\rho} S_z^{*2} - 1\right) Z_o \right]$$

$$\exp\{i\omega(S_x^* x + S_y^* y + S_z^* z - t)\} \qquad (61)$$

The slowness surface for a P wave travelling in the unidirectional fiberglass epoxy composite shown in Fig. 1 is an oblate spheroid. See Fig. 3. Thus, if (x, y, z) are the coordinates of a given point in the medium, there will be only one P wave front passing through it, corresponding to a point (S_x^*, S_y^*, S_z^*) on the slowness surface where the normal is parallel to the given direction. Therefore, it is concluded that for the displacement components along the x, y and z axes, u, v and w, measured by tracing the P wave in the unidirectional fiberglass epoxy composite plate specimen at point M in Fig. 8, there is only one point (S_x^*, S_y^*, S_z^*) on the slowness surface where the normal is parallel to a given direction OM' [5].

3. Directivity Function

The shear stress τ_{yz} and the normal stress τ_{zz} associated with the P wave reaching the point M' in Fig. 8 are used to study their associated directivity functions. The asymptotic shear stress τ_{yz} and the asymptotic normal stress τ_{zz} are obtained by substituting Eqs. (55) through (58) into Eq. (1) and then by setting S_x^* equal to zero as

$$\tau_{zz} \sim \frac{\lambda_n \omega}{2\pi R} \{C_{33} [\frac{-(C_{13}+C_{44})}{\rho} iS_y^* \ S_z^{*2} \ Y_o + (\frac{C_{11}}{\rho} S_y^{*2} + \frac{C_{33}}{\rho} S_z^{*2} - 1) iS_z^* Z_o] + C_{13} [(\frac{C_{44}}{\rho} S_y^{*2} + \frac{C_{33}}{\rho} S_z^{*2} - 1) iS_y^* Y_o) + \frac{-(C_{13}+C_{44})}{\rho} iS_y^{*2} S_z^* Z_o]\}$$

$$\exp\{i\omega(S_y^* y + S_z^* z - t)\} \qquad (62)$$

$$\tau_{yz} \sim \frac{C_{55}\lambda_n \omega}{2\pi R} \{\frac{-(C_{13}+C_{44})}{\rho} iS_y^{*2} S_z^* Y_o + (\frac{C_{11}}{\rho} S_y^{*2} + \frac{C_{33}}{\rho} S_z^{*2} - 1) iS_y^* Z_o + (\frac{C_{44}}{\rho} S_y^{*2} + \frac{C_{33}}{\rho} S_z^{*2} - 1) iS_z^* Y_o) + \frac{-(C_{13}+C_{44})}{\rho} iS_y^* \ S_z^{*2} Z_o\}$$

$$\exp\{i\omega(S_y^* y + S_z^* z - t)\} \qquad (63)$$

The directivity functions associated with the normal stress τ_{zz} in Eq. (62) and the shear stress τ_{yz} in Eq. (63) will be evaluated. Due to the axial symmetry with respect to the zonal axis, the z axis, of the transversely isotropic medium, the values of the directivity functions obtained for the case $S_x = 0$ hold for all values of S_x.

Consider the case of the point load acting along the y direction only; that is, $Y_o \neq 0$ but $X_o = Z_o = 0$ in Eq. (45).

The directivity function D^Y_{yz} of the shear stress τ_{yz} associated with a P wave whose slowness vector is confined to the plane x = 0 is obtained from the amplitude of the shear stress in Eq. (63) by setting $Y_o = R = 1$;

$$D^Y_{yz} = \frac{\lambda_n \omega C_{44} S^*_z}{2\pi} \left(\frac{-C_{13}}{\rho} S^{*2}_y + \frac{C_{33}}{\rho} S^{*2}_z - 1 \right) \tag{64}$$

where λ_n is given in Eq. (57) and is evaluated at the point $(0, S^*_y, S^*_z)$ on the slowness surface for a P wave, Eq. (14); $(0, S^*_y, S^*_z)$ is the point on the slowness surface where the normal is parallel to the given direction and ω is radian frequency. Similarly, the directivity function D^Y_{zz} of the normal τ_{zz} is, from Eq. (62), for $Y_o = R = 1$;

$$D^Y_{zz} = \frac{\lambda_n \omega S^*_y}{2\pi} \left[\frac{C_{13}C_{44}}{\rho} S^{*2}_y - \frac{C_{33}C_{44}}{\rho} S^{*2}_z - C_{13} \right] \tag{65}$$

Next, consider the case of the point load acting along the z direction only; that is, $Z_o \neq 0$, but $X_o = Y_o = 0$ in Eq. (45).

The directivity function D^Z_{yz} of the shear stress τ_{yz} associated with a P wave whose slowness vector is confined to the plane x = 0 is

obtained from the amplitude of the shear stress in Eq. (63) by setting $Z_o = R = 1$;

$$D_{yz}^{Z} = \frac{\lambda_n \omega C_{44} S_y^*}{2\pi} \left(\frac{C_{11}}{\rho} S_y^{*2} + \frac{C_{33}-C_{44}-C_{13}}{\rho} S_z^{*2} - 1 \right) \qquad (66)$$

Similarly, the directivity function D_{zz}^{Z} of the normal stress τ_{zz} is, from Eq. (62), for $Z_o = R = 1$;

$$D_{zz}^{Z} = \frac{\lambda_n \omega S_z^*}{2\pi} \left(\frac{C_{11}C_{33}-C_{13}C_{44}-C_{13}^2}{\rho} S_y^{*2} + \frac{C_{33}^2}{\rho} S_z^{*2} - C_{33} \right) \qquad (67)$$

The polar diagrams for the directivity functions of the shear stress τ_{yz} and the normal stress τ_{zz} (D_{yz}^{Y}, D_{zz}^{Y}, D_{yz}^{Z} and D_{zz}^{Z} given in Eqs. (64) through (67)) associated with the P waves propagating in the unidirectional fiberglass epoxy composite shown in Fig. 1 are obtained by substituting Eq. (35) into Eqs. (64) through (67) at frequencies of 0.75, 1.50 and 2.25 MHz.

Numerical results are shown in Figs. 12 through 23 where the angle of incidence θ given in Eq. (36) is used to determine the direction for which the value of a point $(0, S_y^*, S_z^*)$ on the slowness surface where the normal is parallel to the given direction is thus obtained.

4. Assumptions on the Transducers

The non-contact transmitting transducer in Fig. 7 is assumed to transform an electrical voltage into a uniform stress; however, the non-contact receiving transducer in Fig. 7 transforms a displacement into an electrical voltage. The approach below is similar to that given in [7].

Referring to Fig. 7, if an input voltage of amplitude V and frequency ω is applied according to

$$V_i(t) = Ve^{-i\omega t} \tag{68}$$

the stress σ that is introduced into the specimen plate by the non-contact transmitting transducer is

$$\sigma(t) = F_1(\omega)Ve^{-i(\omega t + \phi_1)} \tag{69}$$

where $F_1(\omega)$ is the transduction ratio for the non-contact transmitting transducer in transforming a voltage to a stress and ϕ_1 is a phase angle. In Eqs. (68) and (69), the harmonic character of the signals is expressed in the complex notation where $i = \sqrt{-1}$ and only the real parts of these and subsequent equations should be considered. Thus, the amplitude T of the applied force is defined as

$$T = F_1(\omega)V \tag{70}$$

Similarly, if a stress wave producing a displacement d of amplitude D and frequency ω that is detected by the non-contact receiving transducer is defined as

$$d(t) = De^{-i\omega t} \tag{71}$$

the output voltage from the non-contact receiving transducer, see Fig. 7, is

$$V_o(t) = F_2(\omega)De^{-i(\omega t + \phi_2)} \tag{72}$$

where $F_2(\omega)$ is the transduction ratio for the non-contact receiving transducer in transforming a displacement to a voltage, and ϕ_2 is a phase angle. Thus, the amplitude V′ of the output electrical voltage is

$$V' = F_2(\omega)D \tag{73}$$

The characteristics of $F_1(\omega)$ and $F_2(\omega)$ are unknown except that the dimensions of the product $F_1(\omega)F_2(\omega)$ are $[kg/m^2 \cdot sec^2]$.

5. Steady-State Output Voltage Amplitude due to Multiple Wave Reflections in a Plate

Since the P wave traced in the unidirectional fiberglass epoxy composite plate specimen shown in Fig. 8 is travelling in the y-z plane, it follows from Eqs. (59), (60) and (61) that only the displacement components along the y and z axes, v and w, are detectable at the point M'. Consider first the point load acting along the y direction only; that is, $Y_o \neq 0$, but $X_o = Z_o = 0$ in Eq. (45).

The amplitude of the y-component displacement D_v^Y evaluated at the point M' can be obtained from Eqs. (37) and (60) as

$$D_v^Y = \frac{f_1(S_y^*, S_z^*)}{R_n} Y_o \tag{74}$$

where $f_1(S_y^*, S_z^*) = (\lambda_n/2\pi)\left|(C_{44}/\rho)S_y^{*2} + (C_{33}/\rho)S_z^{*2} - 1\right|$. Similarly, the amplitude of the z-component displacement D_w^Y evaluated at the point M' can be obtained from Eqs. (37) and (61) as

$$D_w^Y = \frac{f_2(S_y^*, S_z^*)}{R_n} Y_o \tag{75}$$

where $f_2(S_y^*, S_z^*) = (\lambda_n/2\pi)[(C_{13}+C_{44})/\rho]S_y^* S_z^*$.

Next, consider the point load acting along the z-direction only; that is, $Z_o \neq 0$, but $X_o = Y_o = 0$ in Eq. (45).

The amplitude of the y-component displacement D_v^Z evaluated at the point M' can be obtained from Eqs. (37) and (60) as

$$D_v^Z = \frac{f_2(S_y^*, S_z^*)}{R_n} Z_o \tag{76}$$

evaluated at the point M' can be obtained from Eqs. (37) and (61) as

$$D_w^Z = \frac{f_3(S_y^*, S_z^*)}{R_n} Z_o \tag{77}$$

where $f_3(S_y^*, S_z^*) = (\lambda_n/2\pi)\left|(C_{11}/\rho)S_y^{*2} + (C_{33}/\rho)S_z^{*2} - 1\right|$.

Finally, consider the point load acting along the x direction only; that is, $X_o \neq 0$, but $Y_o = Z_o = 0$ in Eq. (45). It follows from Eqs. (60) and (61) that the amplitude of the y-component displacement and the amplitude of the z-component displacement vanish at the point M'. This is due to the fact that the P wave is travelling in the y-z plane.

According to Eqs. (74) through (77), the amplitude of a displacement component at the point M', denoted as $D_{M'}$, can be expressed in

the following form as

$$D_{M'} = \frac{f_i(S_y^*, S_z^*)}{R_n} T \tag{78}$$

where T is the applied point load and is equivalent to either Y_o or Z_o in Eqs. (74) through (77); and $f_i(S_y^*, S_z^*)$ (i=1,2 or 3) is determined from one of the Eqs. (74) through (77), depending on which displacement component is measured and along which direction the point load is applied.

However, with the bottom boundary present, the wave is reflected a total of (2n-1) times, as shown in Fig. 8. Thus, the amplitude of displacement at the point M is D_M and is expressed as

$$D_M = Q_{pp}^{2n-1} D_{M'} \tag{79}$$

where Q_{pp} is the amplitude ratio of the reflected P wave to the incident P wave, as shown in Fig. 5, and is a function of the angle of incidence θ defined in Eq. (36).

Here, we have ignored the effects of mode conversion. The amplitude of the output voltge from the non-contact receiving transducer is V' and can be obtained by substituting Eqs. (78) and (79) into Eq. (73) as

$$V' = \frac{F_2(\omega)\ Q_{pp}^{2n-1}\ f_i(S_y^*, S_z^*)T}{R_n} \tag{80}$$

Substitution of Eq. (70) into Eq. (80) gives

$$V' = \frac{F_1(\omega)\ F_2(\omega)\ Q_{pp}^{2n-1}\ f_i(S_y^*,\ S_z^*)V}{R_n} \tag{81}$$

Introducing the P wave attenuation constant α of the unidirectional fiberglass epoxy composite and a possible electrical signal amplification factor K, Eq. (81) can be written as

$$V' = KF_1(\omega)F_2(\omega)Q_{pp}^{2n-1}f_i(S_y^*,\ S_z^*)V\ \frac{e^{-\alpha R_n}}{R_n} \tag{82}$$

Eq. (82) gives the output voltage amplitude from the non-contact receiving transducer due to an input voltage amplitude V at the non-contact transmitting transducer when the P wave path has undergone n reflections from the bottom face of the unidirectional fiberglass epoxy composite plate specimen, as shown in Fig. 8.

DISCUSSION AND CONCLUSION

In the acousto-ultrasonic input-output characterization of the unidirectional fiberglass epoxy composite plate specimen, the angle of reflection of the reflected P wave is equal to the angle of incidence of the incident P wave for each reflection at either the top or the bottom face of the plate. This is due to the fact that the isotropic plane is parallel to both faces of the plate. However, if the parallelism between the isotropic plane and the plane boundaries where reflection occurs does not exist, the angle of reflection is not equal to the angle of incidence. In this case, the use of a semi-infinite transversely isotropic medium, neglecting the existence of the bottom face of the plate specimen except for the cumulative reflections, to compute the delay time, the displacement and the directivity functions becomes inappropriate.

It is observed from Fig. 9 that an increase in the number of reflections n results in a minor increase in the delay time t_n at each value of the dimensionless separation ℓ/h. For a given plate thickness h and a given the separation distance ℓ between the transmitting transducer and the receiving transducer, an increase in the number of reflections n results in a decrease in the angle of incidence θ, as given by Eq. (36), thereby increasing the travelling distance R_n, from Eq. (37). The phase velocity C_1 of a P wave in

the unidirectional fiberglass epoxy composite increases with decreasing angle of θ, as shown in Fig. 10. For the time delay, the increase in the travelling distance R_n is partly offset by the increase in the phase velocity C_1 with an increse in the number of reflections n. This accounts for the minor increase in the delay time given by Eq. (38). However, in an isotropic medium, the phase velocity of a stress wave is directionally independent. As a result, the increase in the dealy time t_n caused by an increase in the number of reflections n is solely attributed to the increase in the travelling distance R_n in an isotrpic plate. Therefore, it is concluded that the directional dependence of the phase velocity of a stress wave travelling in a transversely isotropic medium has a significant effect on the delay time when conducting acousto-ultrasonic testing.

Now, consider the case of a given number of reflections n. An increase in the separation distance ℓ results in an increase in the travelling distance R_n, as shown in Fig. 8, and an increase in the angle of incidence θ given by Eq. (36). An increasing angle of incidence θ results in a decreasing phase velocity C_1, as shown in Fig. 10. Consequently, the delay time t_n increases sharply as a result of the increasing separation distance ℓ for a given number of reflections n, as shown in Fig. 10. However, as the separation distance ℓ approaches infinity, the phase velocity approaches a limit. Thus, (for $\ell/h \to \infty$) the increase in the delay time t_n is due solely to

the increase in the travelling distance R_n, which is similar to the isotropic medium case.

This theoretical investigation provides a step forward in the quantitative understanding of acousto-ultrasonic nondestructive evaluation (NDE) parameters such as stress wave factor (SWF) in transversely iostropic media. It also provides the potential for assisting in the development of more efficient and more revealing NDE schems utilizing wave propagation.

REFERENCES

[1] E. R. C. Marques and J. H. Williams, Jr., "Stress Waves in Transversely Isotropic Media," Composite Materials and Nondestructive Evaluation Laboratory, MIT, May 1986.

[2] E. G. Henneke II, "Reflection-Refraction of a Stress Wave at a Plane Boundary between Anisotropic Media," Journal of the Acoustical Society of America, Vol. 51, Part 2, April 1972, pp. 210-217.

[3] M. J. P. Musgrave, " On the Propagation of Elastic Waves in Aeolotropic Media," Proceedings of the Royal Society of London, Series A, Vol. 226, 1954, pp. 339-355.

[4] M. J. P. Musgrave, " Reflection and Refraction of Plane Elastic Waves at a Plane Boundary between Anisotropic Media," Journal of Geophysics, Vol.3, 1960, pp. 406-418.

[5] V. T. Buchwald, "Elastic Waves in Anisotropic Media," Proceedings of the Royal Society, Series A, Vol. 253, 1959, pp. 563-580.

[6] J. H. Williams, Jr., E. R. C. Marques and S. S. Lee, "Wave Propagation in Anisotropic Infinite Medium Due to an Oscillatory Point Source with Application to a Unidirectional Composite Material," Composite Materials and Nondestructive Evaluation Laboratory, MIT, May 1986.

[7] J. H. Williams, Jr., H. Karagulle, and S. S. Lee, " Ultrasonic Input-Output for Transmitting and Receiving Longitudinal Transducers Coupled to Same Face of Isotropic Elastic Plate," Materials Evaluation, Vol. 40, May 1982, pp. 655-662.

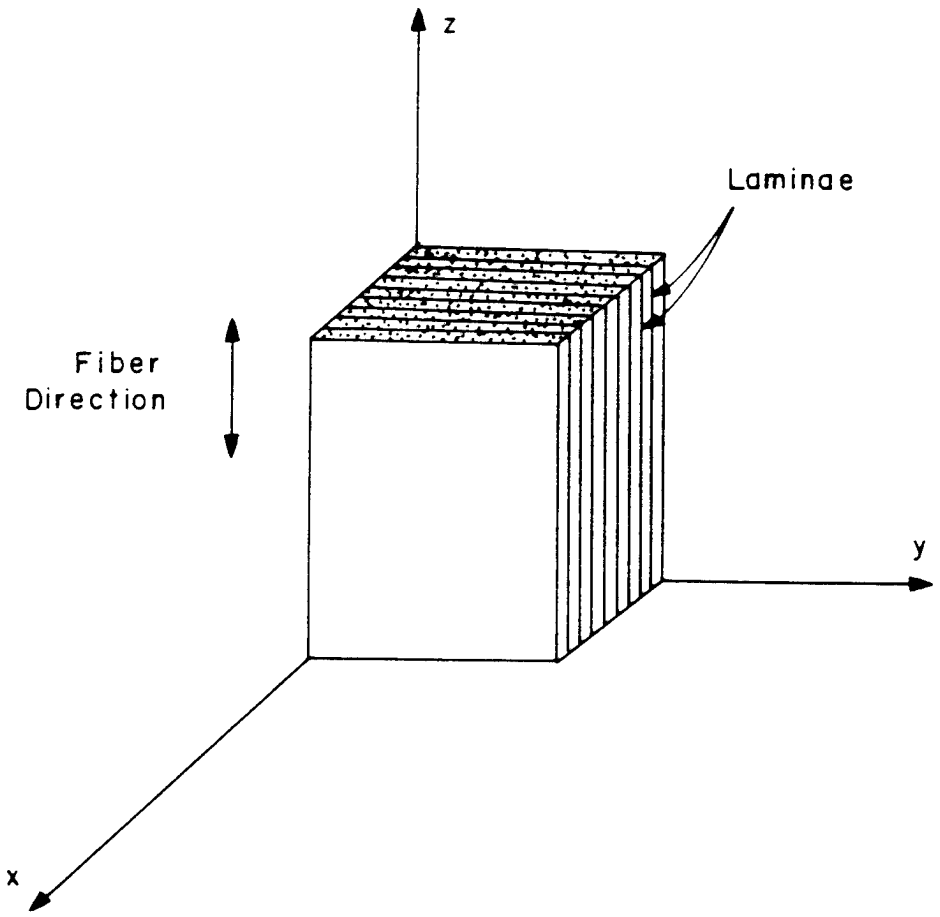

Fig. 1 Unidirectional fiber reinforced composite modelled as transversely isotropic medium.

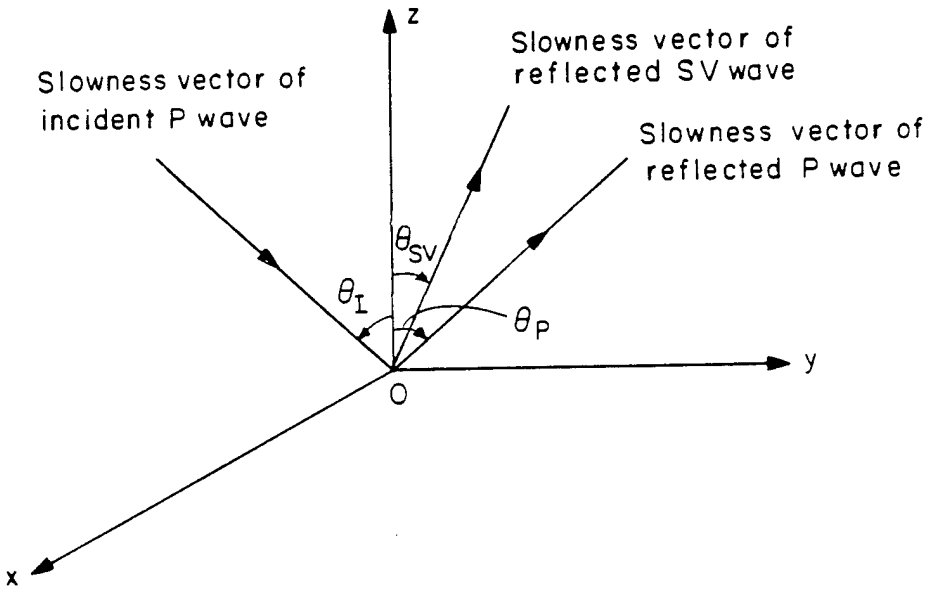

Fig. 2 Coordinate system (x,y,z) in analysis of single reflection problem at stress-free plane boundary of semi-infinte transversely isotropic medium; $z = 0$ is plane boundary where single reflection occurs, $z < 0$ is free space, and $x = 0$ is plane of incidence.

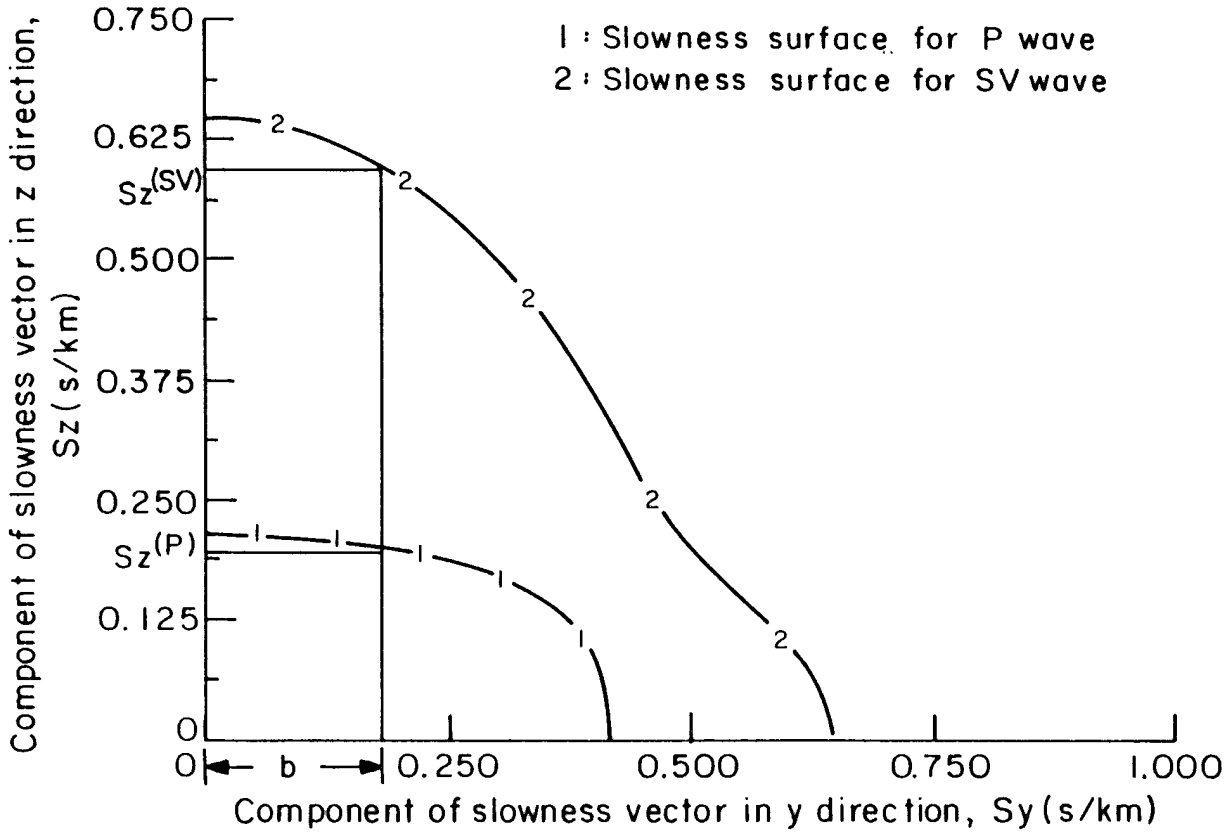

Fig. 3 Two sheets of slowness surfaces for P and SV waves in unidirectional fiberglass epoxy composite for positive y-z quadrant.

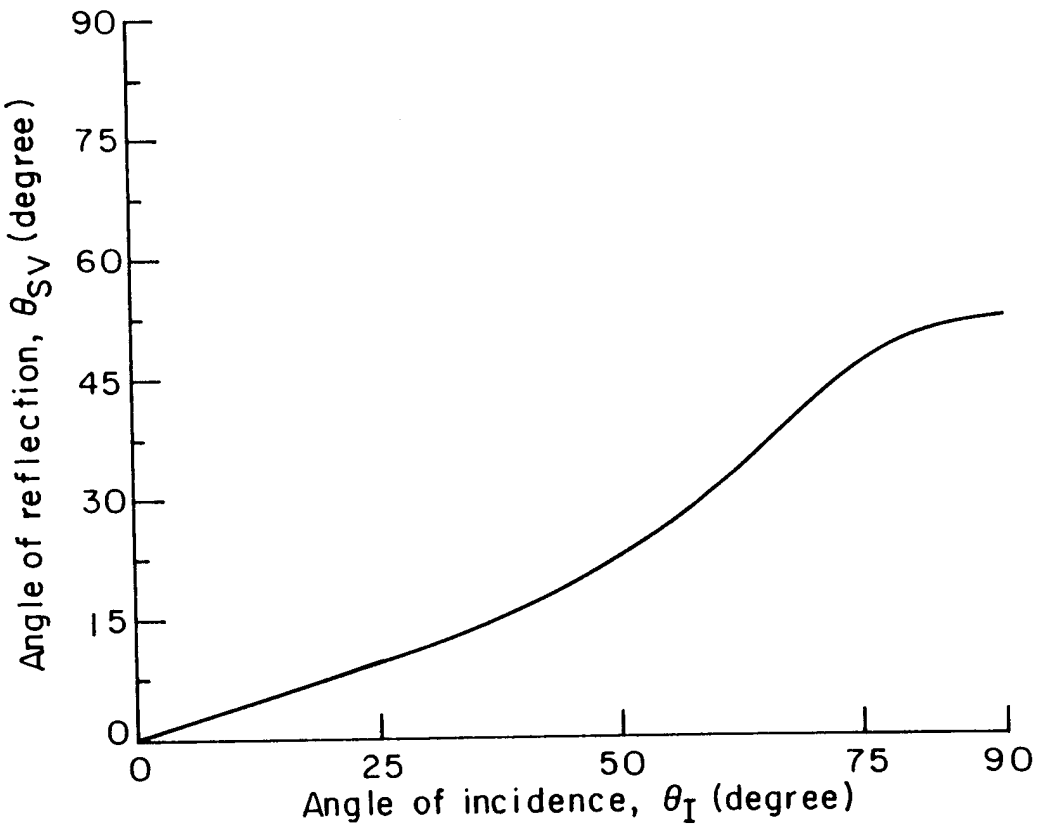

Fig. 4 Angle of reflection of reflected SV wave versus angle of incidence of incident P wave in unidirectional fiberglass epoxy composite.

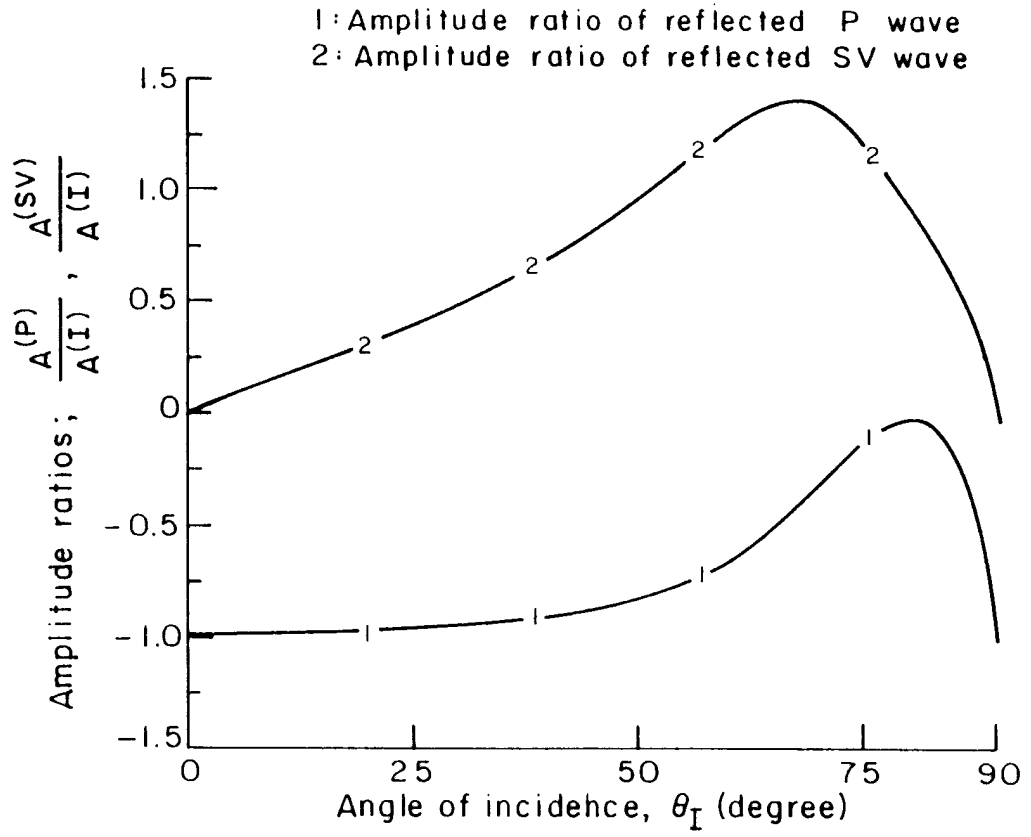

Fig. 5 Amplitude ratios of reflected P and SV waves to incident P wave versus angle of incidence of incident P wave in unidirectional fiberglass epoxy composite.

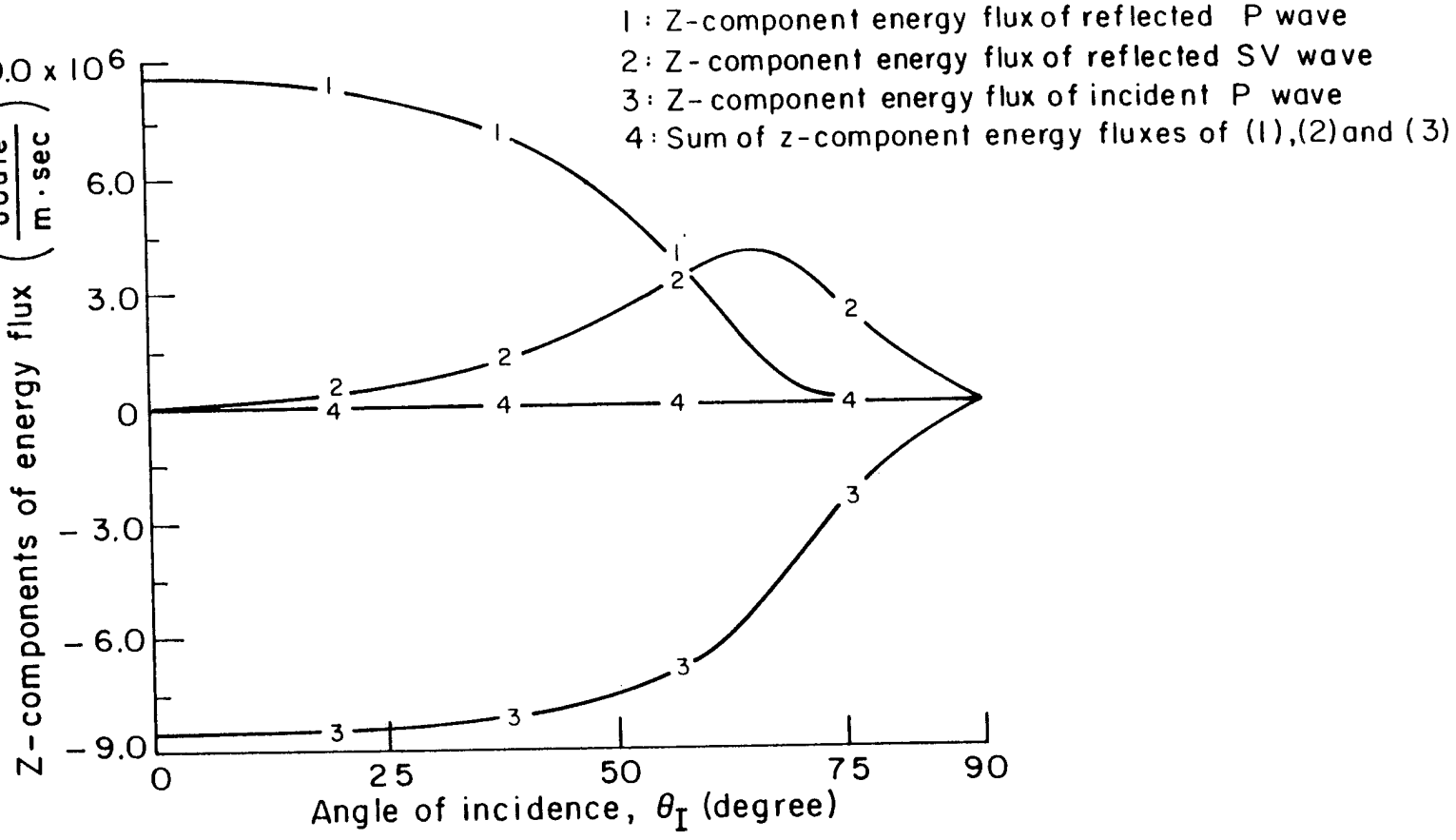

Fig. 6 Energy fluxes normal to plane boundary, assuming radian frequency equal to unity, for incident P wave in unidirectional fiberglass epoxy composite.

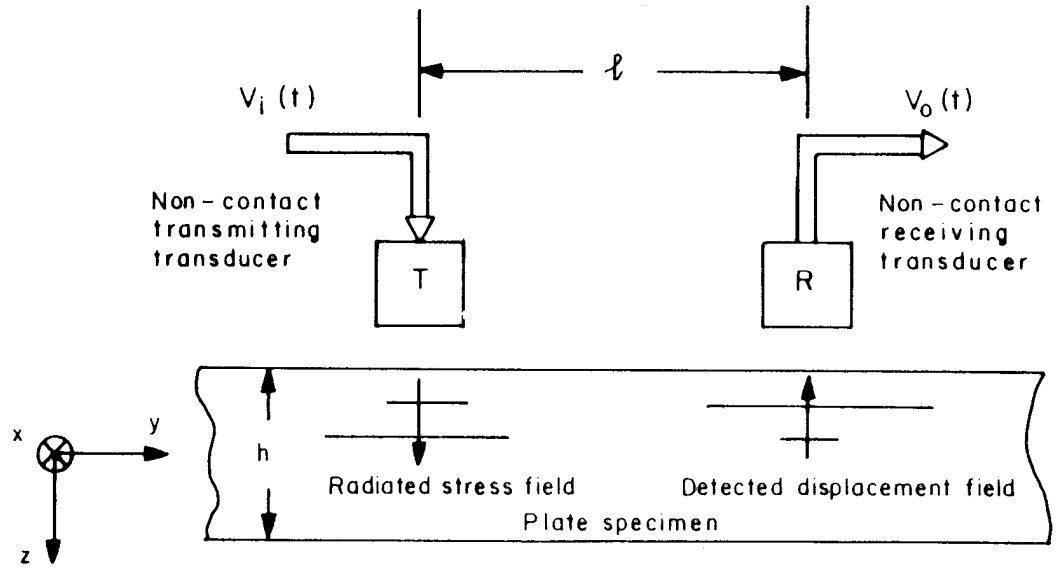

Fig. 7 Schematic of non-contact acousto-ultrasonic test configuration.

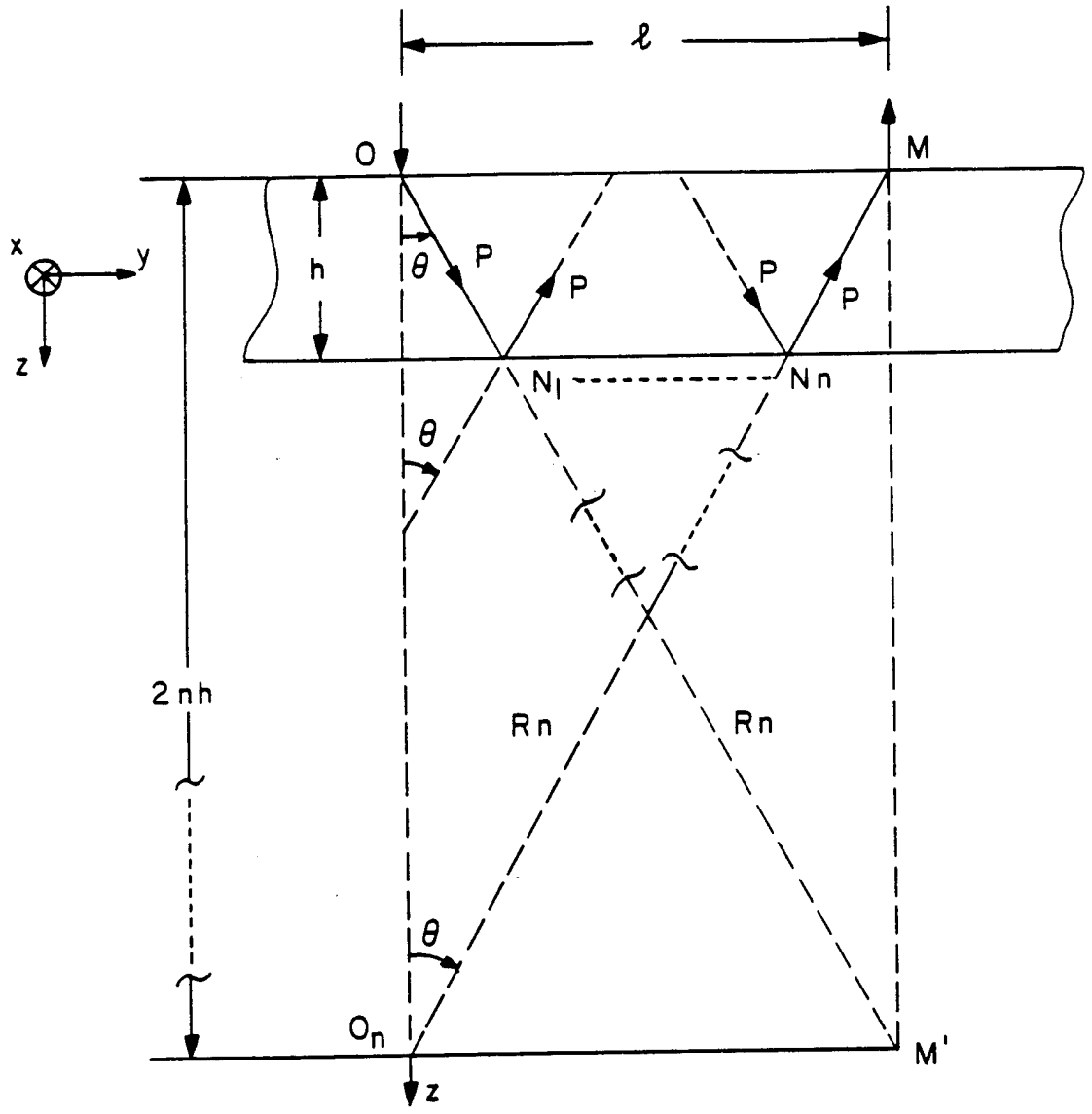

Fig. 8 Path of P-P-... wave which arrives at point M after n reflections from bottom boundary.

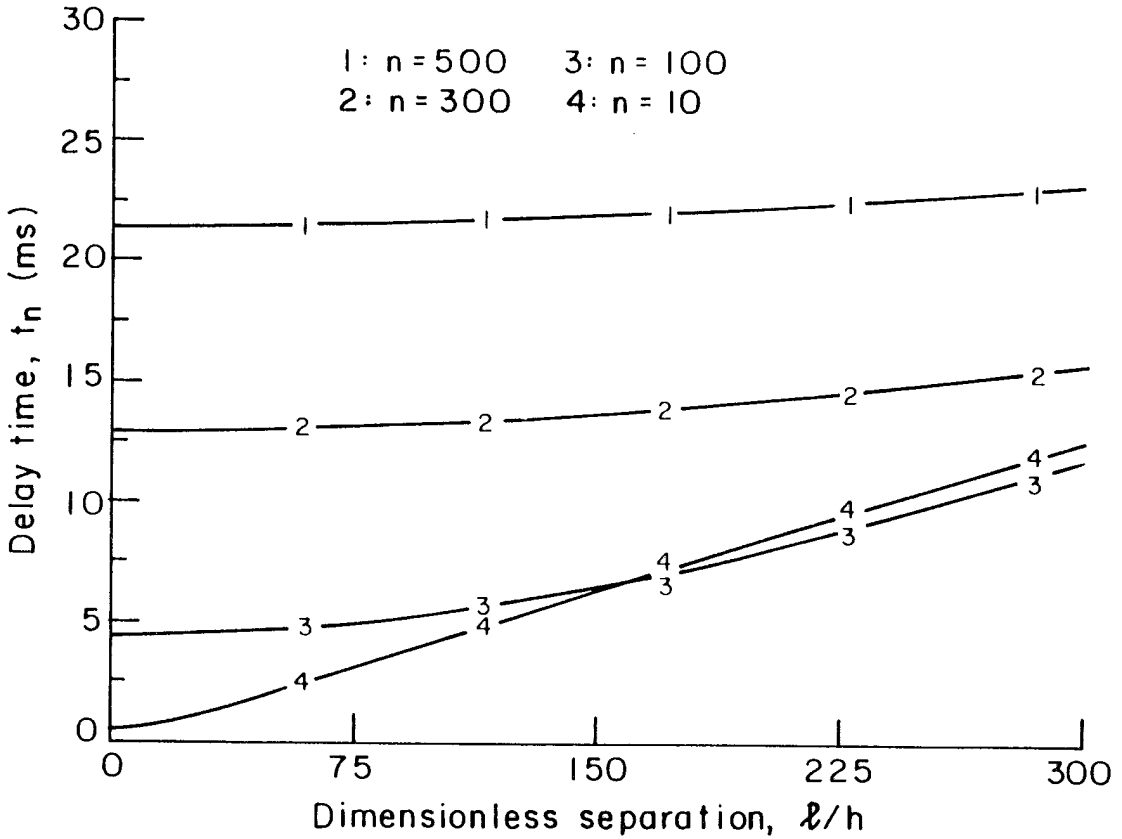

Fig. 9 Delay time versus dimensionless separation (ℓ/h) with number of reflections n, from bottom face of fiberglass epoxy composite plate specimen, as parameter.

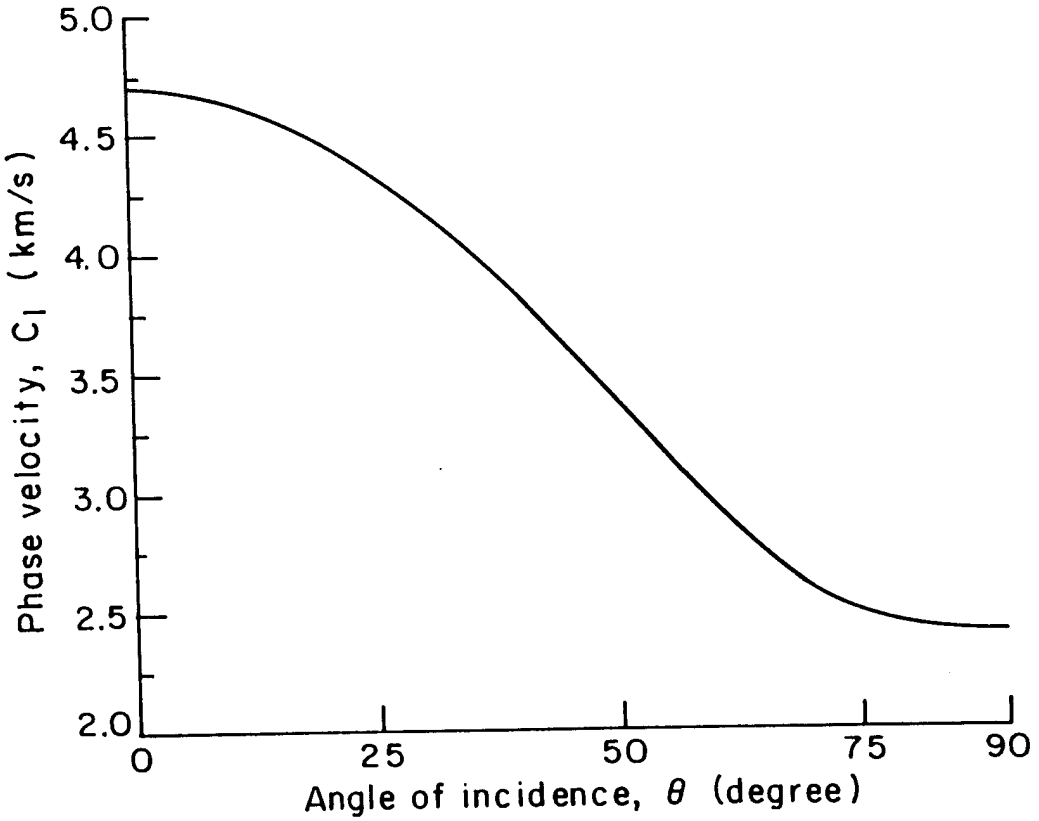

Fig. 10 Phase velocity versus angle of incidence for P wave in unidirectional fiberglass epoxy composite plate specimen.

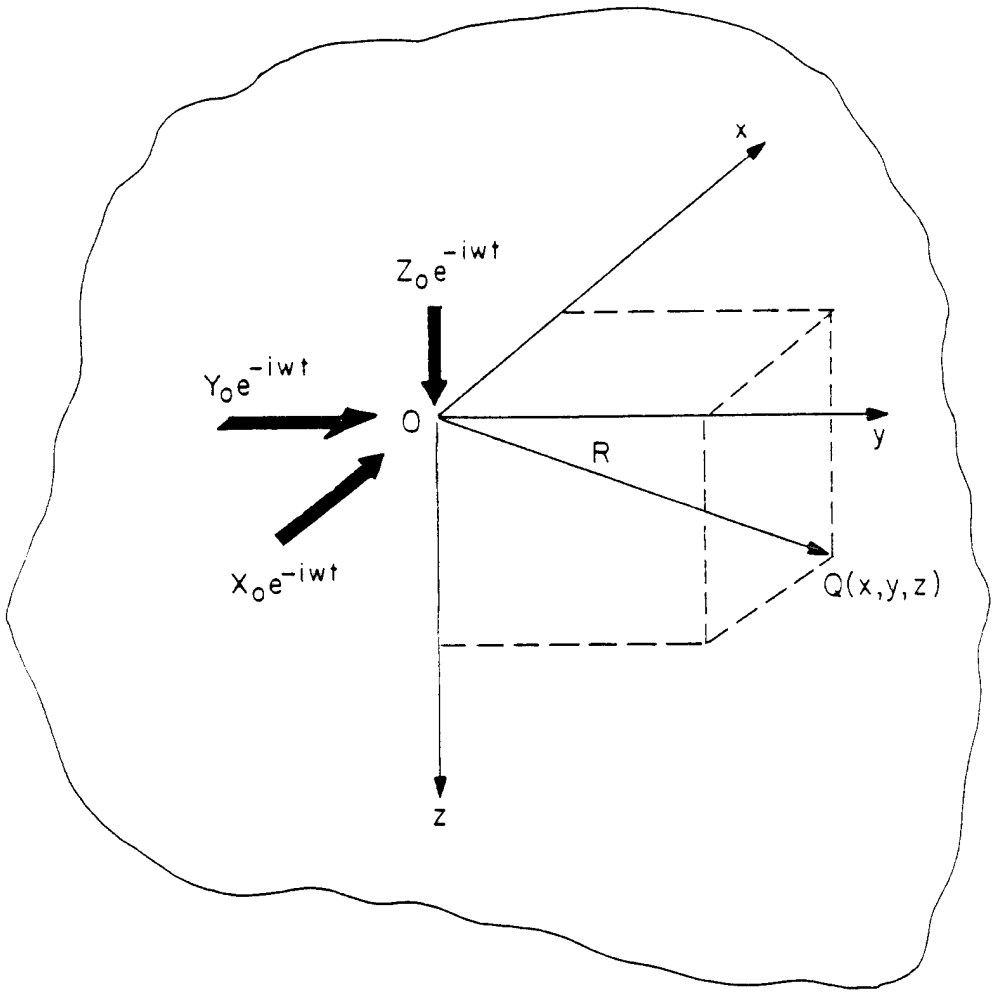

Fig. 11 Schematic illustrating sinusoidal point load exciting infinite transversely isotropic medium, where xy plane is isotropic plane in cartesian coordinate system defined by O(x,y,z).

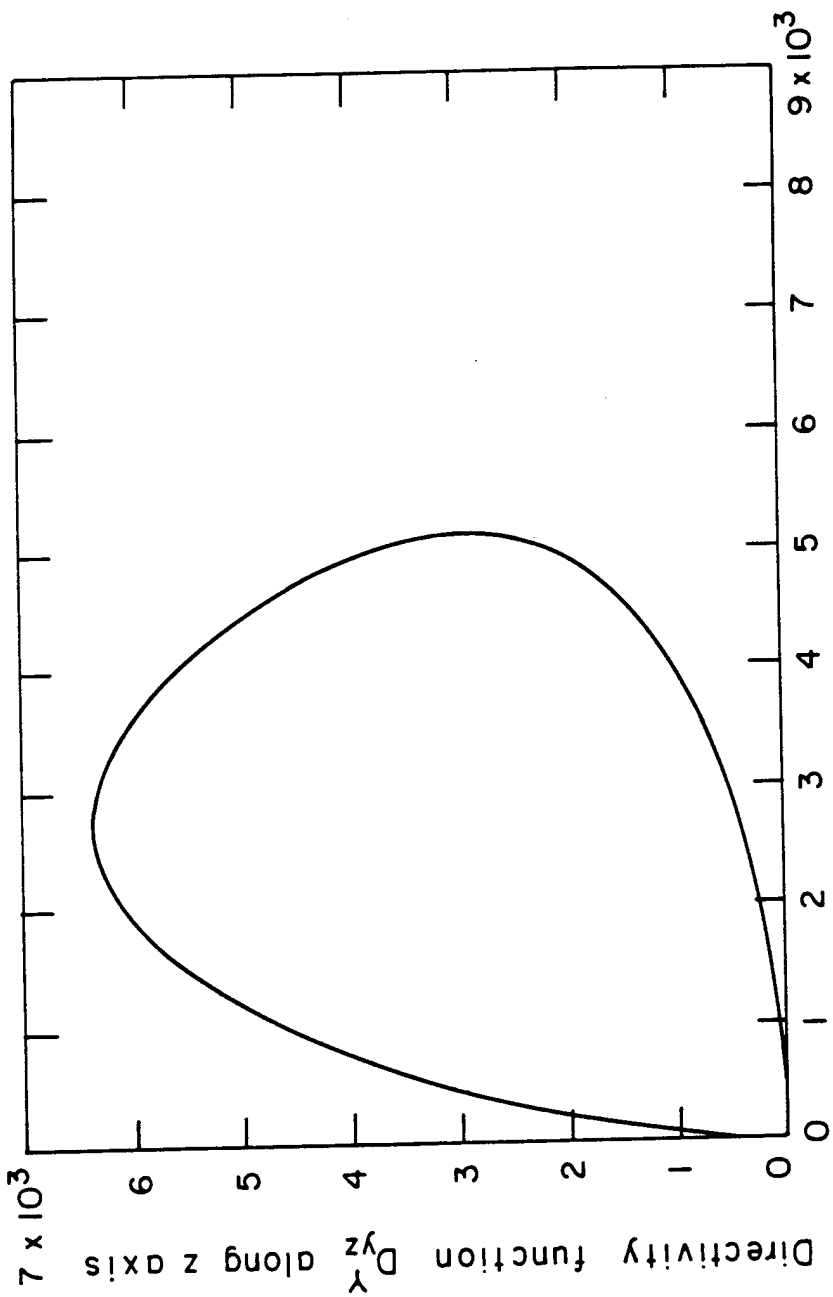

Fig. 12 Polar diagram for directivity function D^Y_{yz} of shear stress τ_{yz} at transmitting origin associated with P wave in unidirectional fiberglass epoxy composite at frequency of 0.75 MHz for positive y-z quadrant due to applied point load acting along y-direction.

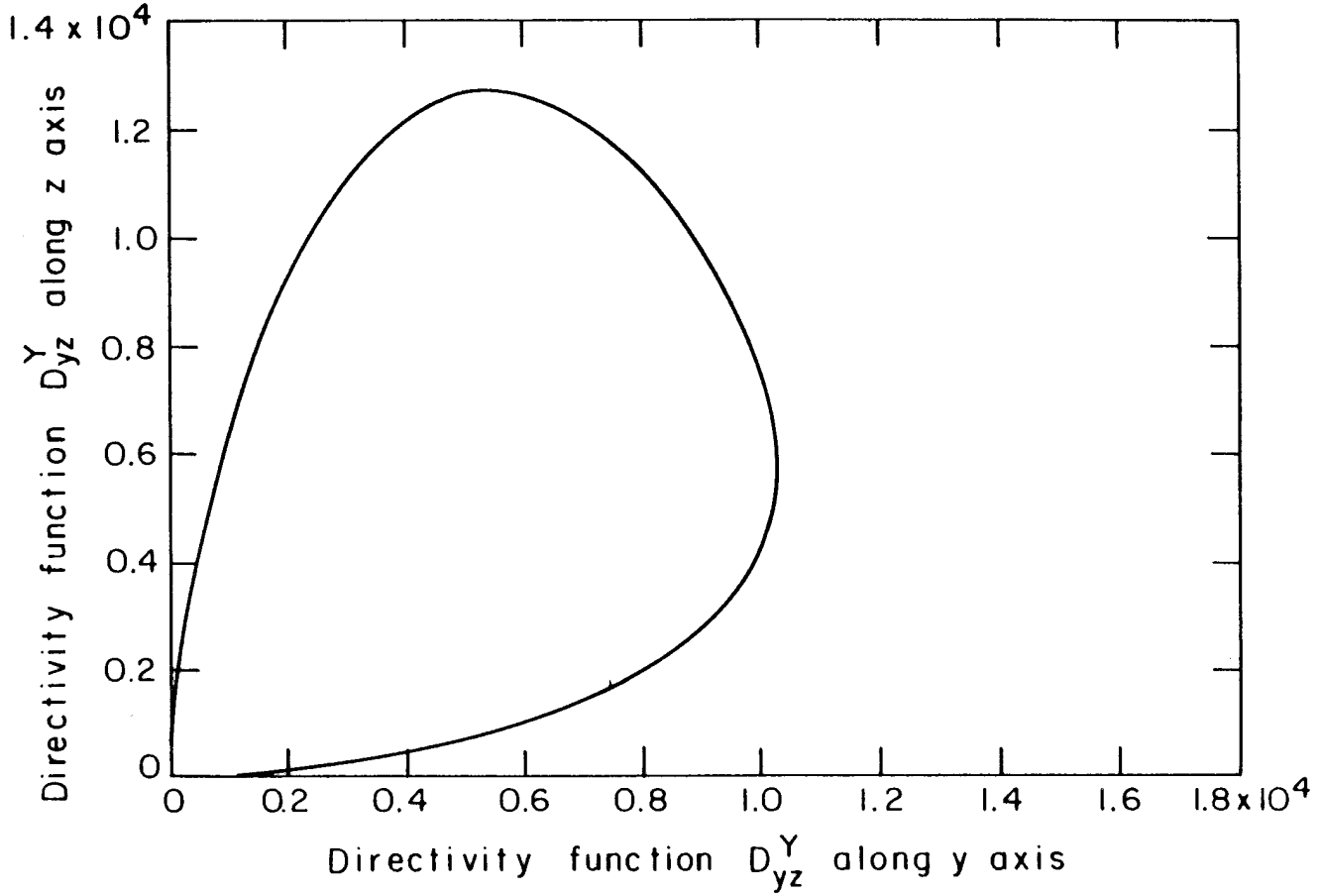

Fig. 13 Polar diagram for directivity function D^{Y}_{yz} of shear stress τ_{yz} at transmitting origin associated with P wave in unidirectional fiberglass epoxy composite at frequency of 1.50 MHz for positive y-z quadrant due to applied point load acting along y-direction.

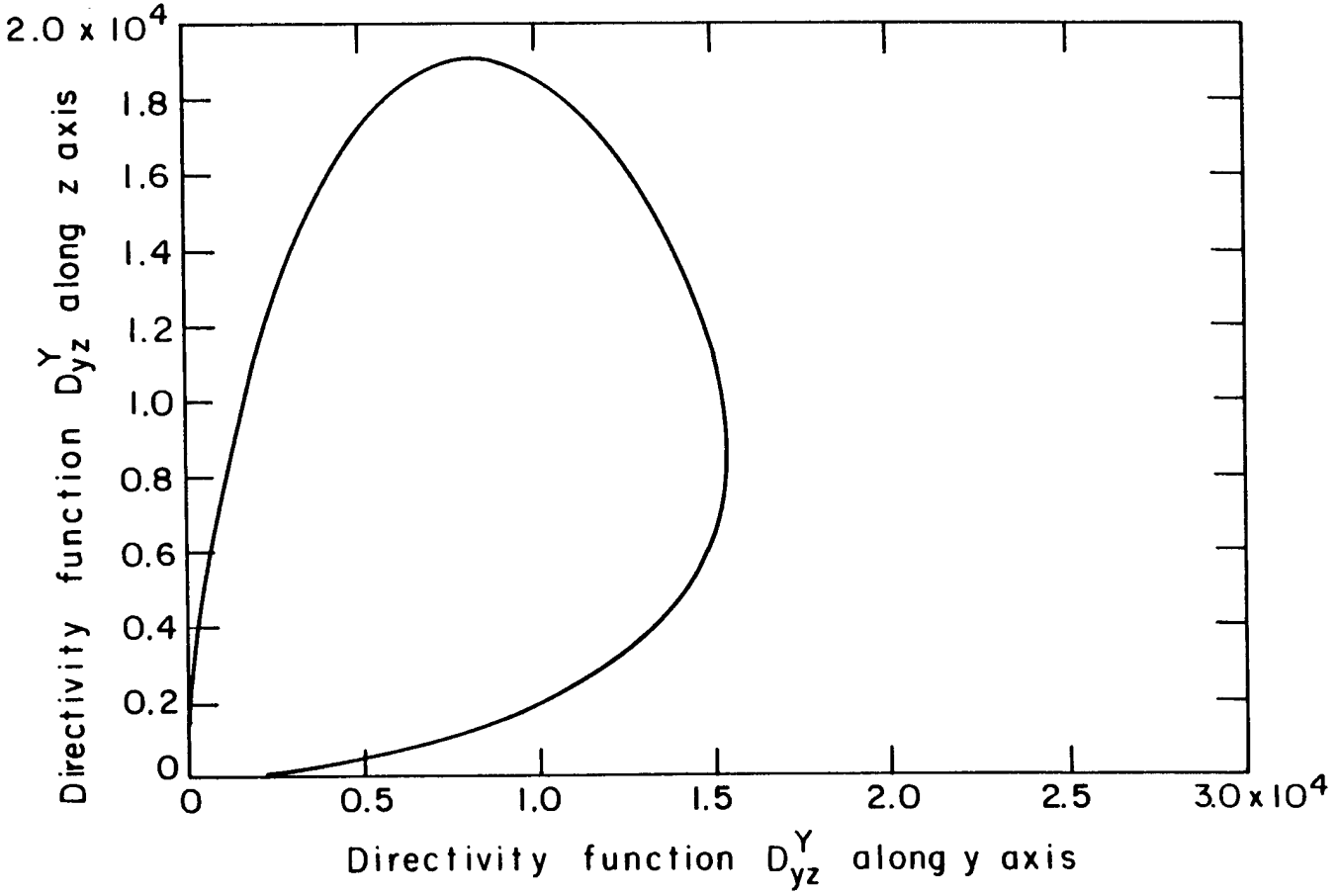

Fig. 14 Polar diagram for directivity function D_{yz}^{Y} of shear stress τ_{yz} at transmitting origin associated with P wave in unidirectional fiberglass epoxy composite at frequency of 2.25 MHz for positive y-z quadrant due to applied point load acting along y-direction.

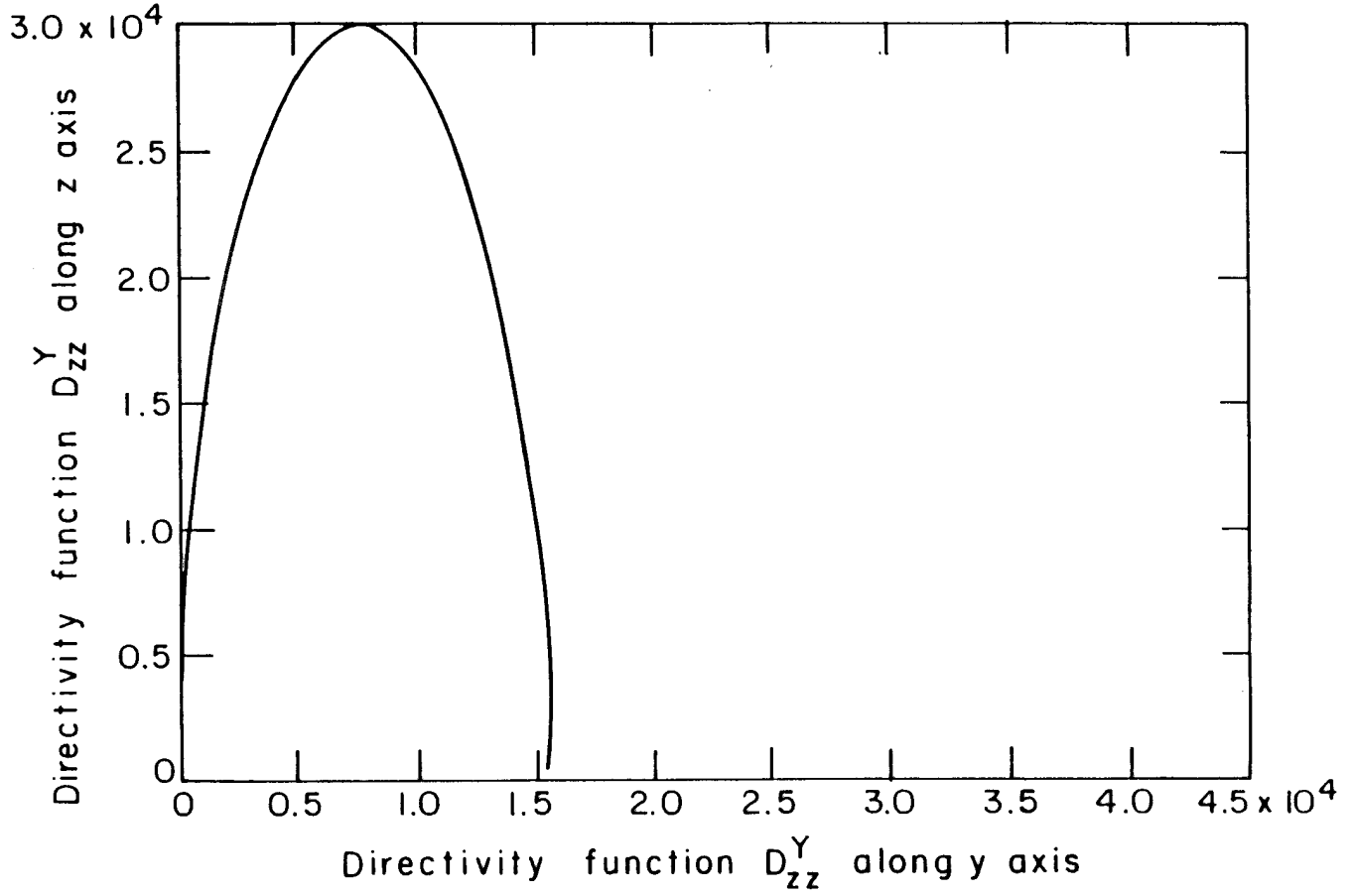

Fig. 15 Polar diagram for directivity function D_{zz}^{Y} of normal stress τ_{zz} at transmitting origin associated with P wave in unidirectional fiberglass epoxy composite at frequency of 0.75 MHz for positive y-z quadrant due to applied point load acting along y-direction.

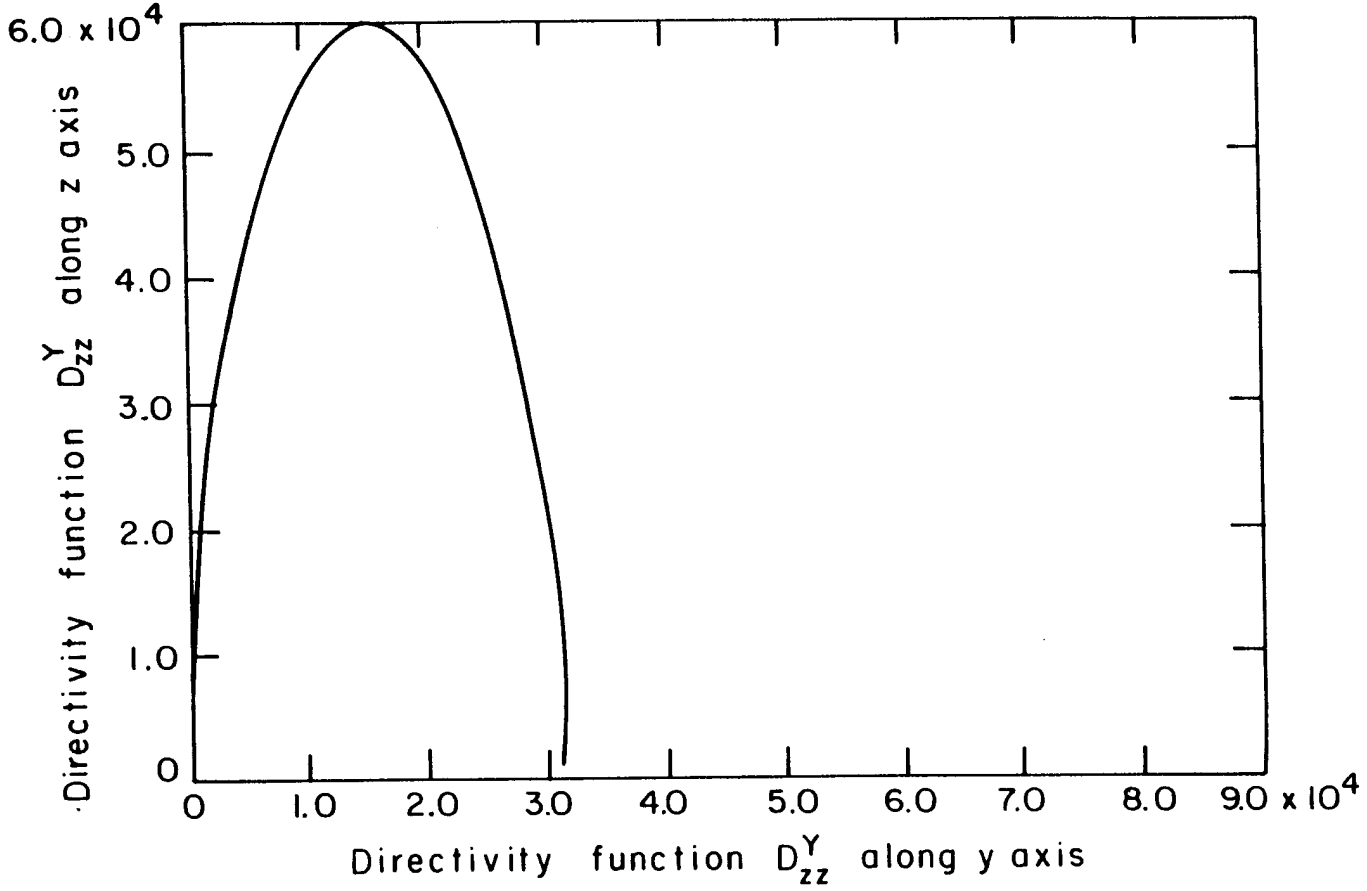

Fig. 16 Polar diagram for directivity function D^Y_{zz} of normal stress τ_{zz} at transmitting origin associated with P wave in unidirectional fiberglass epoxy composite at frequency of 1.50 MHz for positive y-z quadrant due to applied point load acting along y-direction.

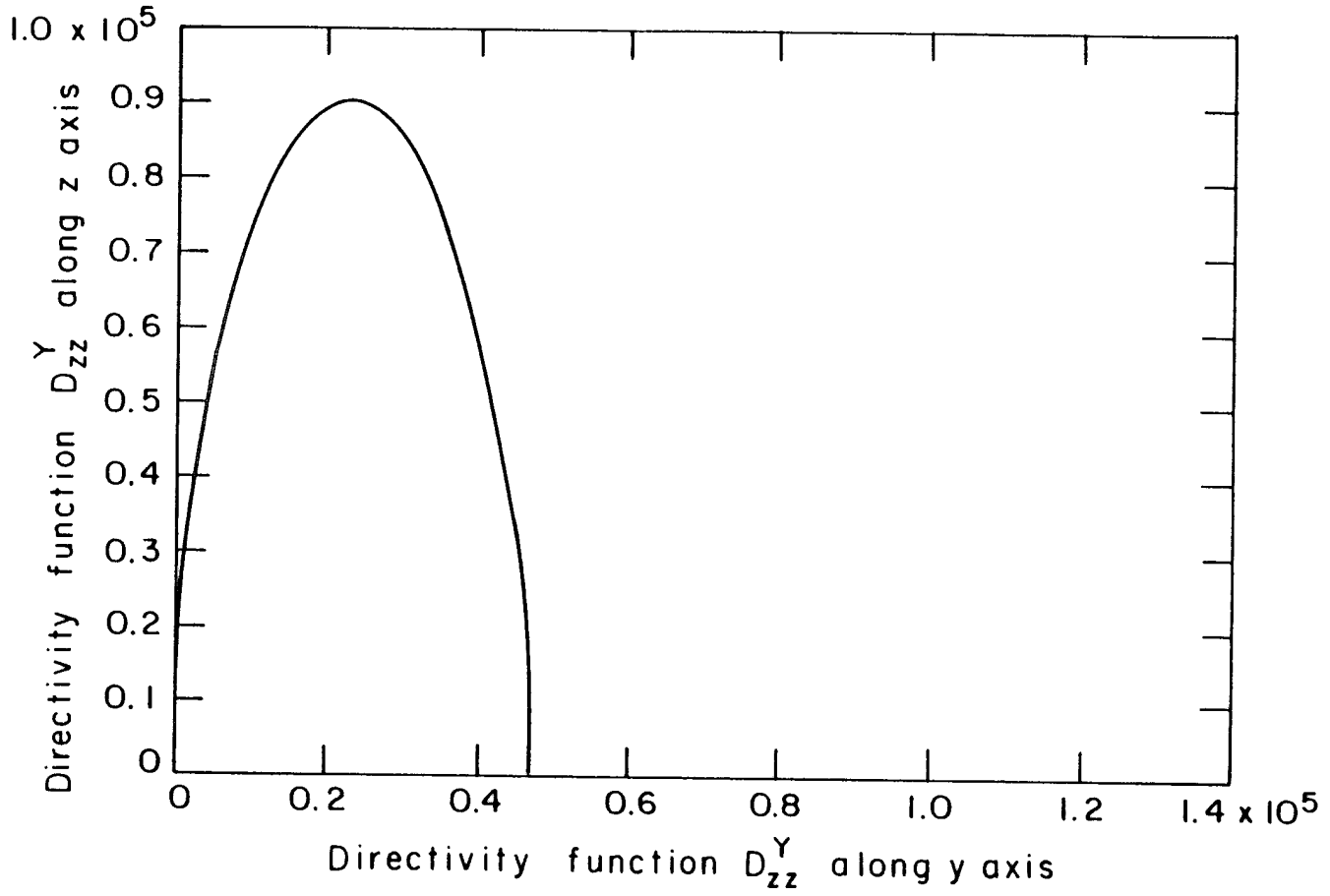

Fig. 17 Polar diagram for directivity function D^{Y}_{zz} of normal stress τ_{zz} at transmitting origin associated with P wave in unidirectional fiberglass epoxy composite at frequency of 2.25 MHz for positive y-z quadrant due to applied point load acting along y-direction.

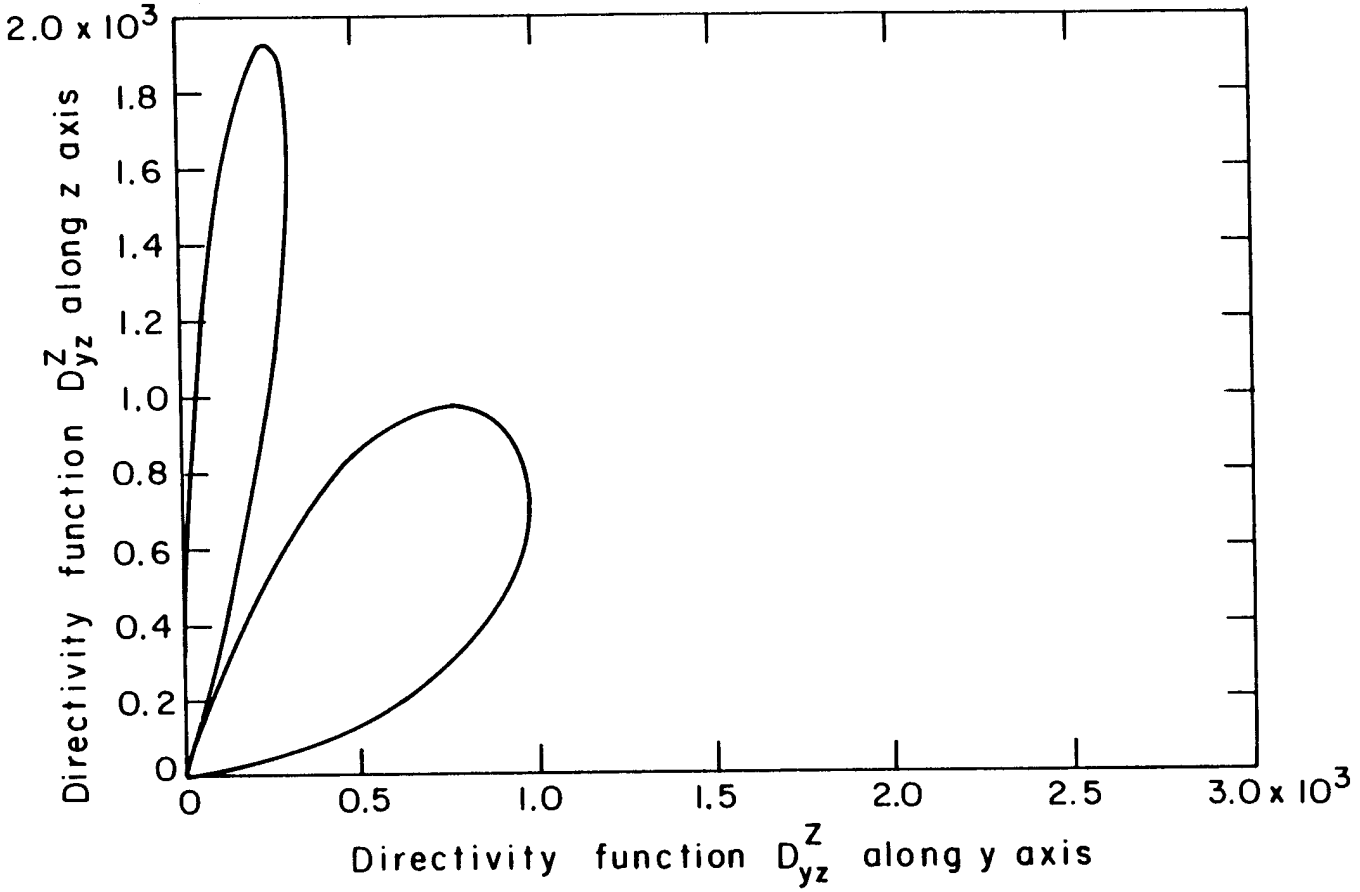

Fig. 18 Polar diagram for directivity function D_{yz}^{z} of shear stress τ_{yz} at transmitting origin associated with P wave in unidirectional fiberglass epoxy composite at frequency of 0.75 MHz for positive y-z quadrant due to applied point load acting along z-direction.

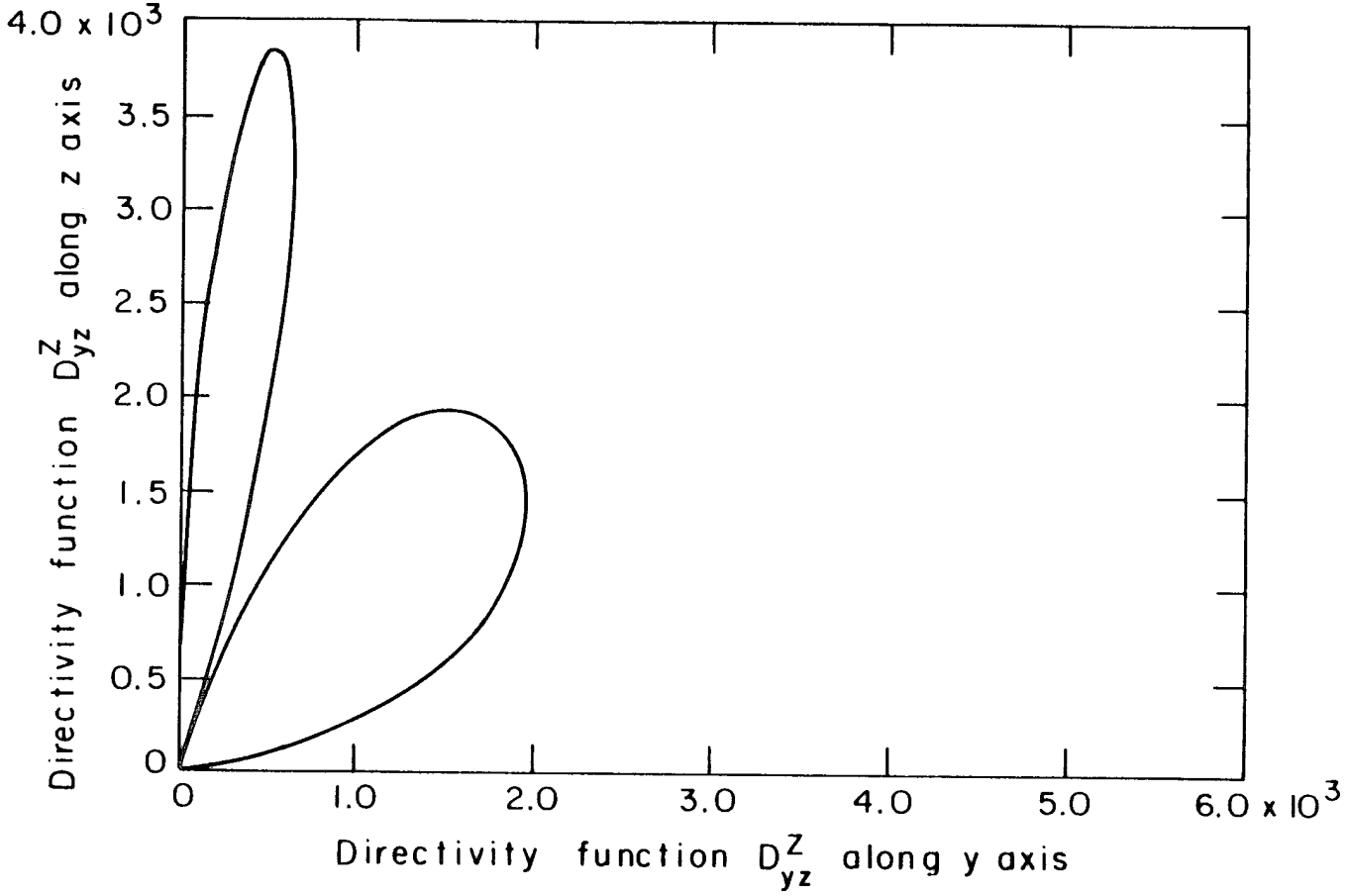

Fig. 19 Polar diagram for directivity function D_{yz}^{z} of shear stress τ_{yz} at transmitting origin associated with P wave in unidirectional fiberglass epoxy composite at frequency of 1.50 MHz for positive y-z quadrant due to applied point load acting along z-direction.

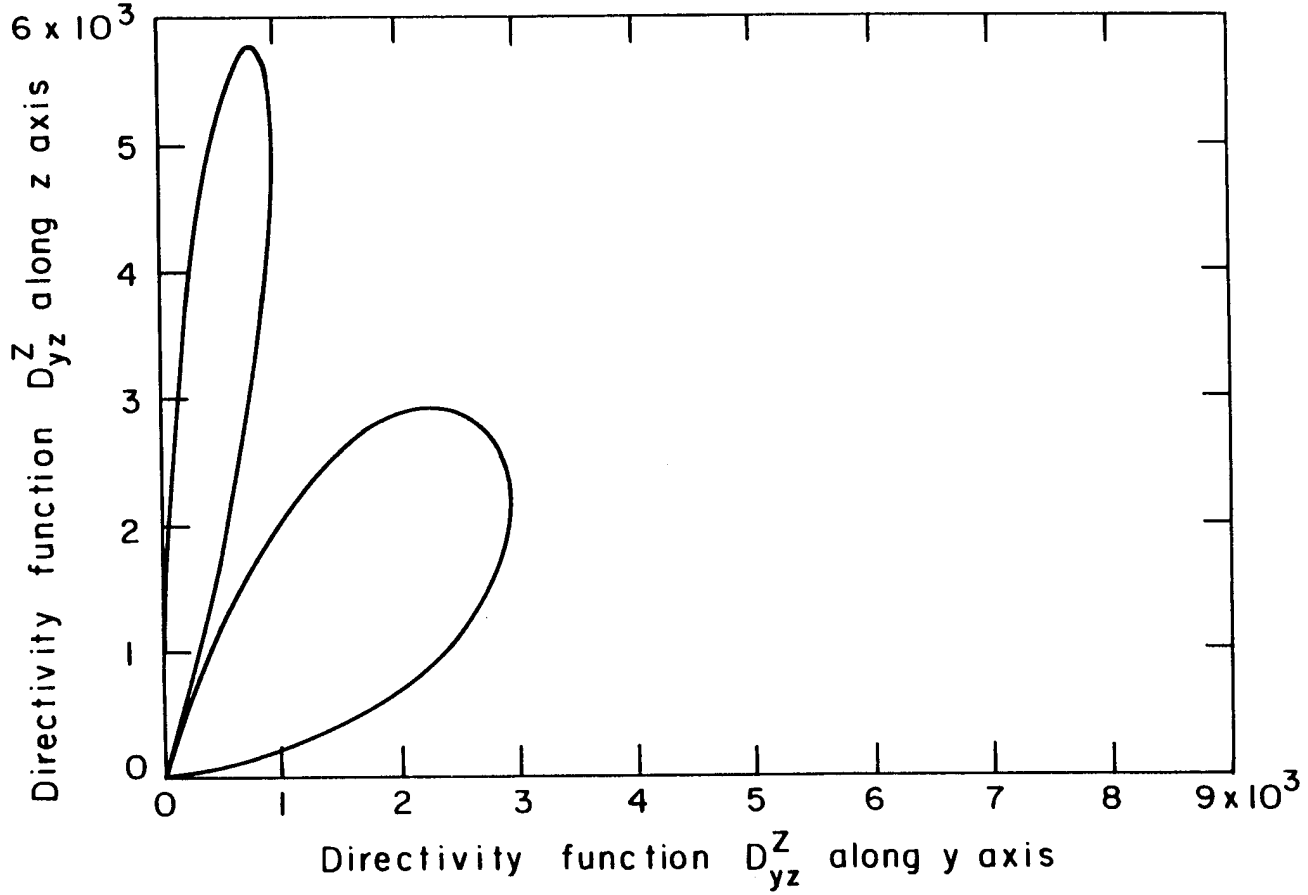

Fig. 20 Polar diagram for directivity function D_{yz}^{z} of shear stress τ_{yz} at transmitting origin associated with P wave in unidirectional fiberglass epoxy composite at frequency of 2.25 MHz for positive y-z quadrant due to applied point load acting along z-direction.

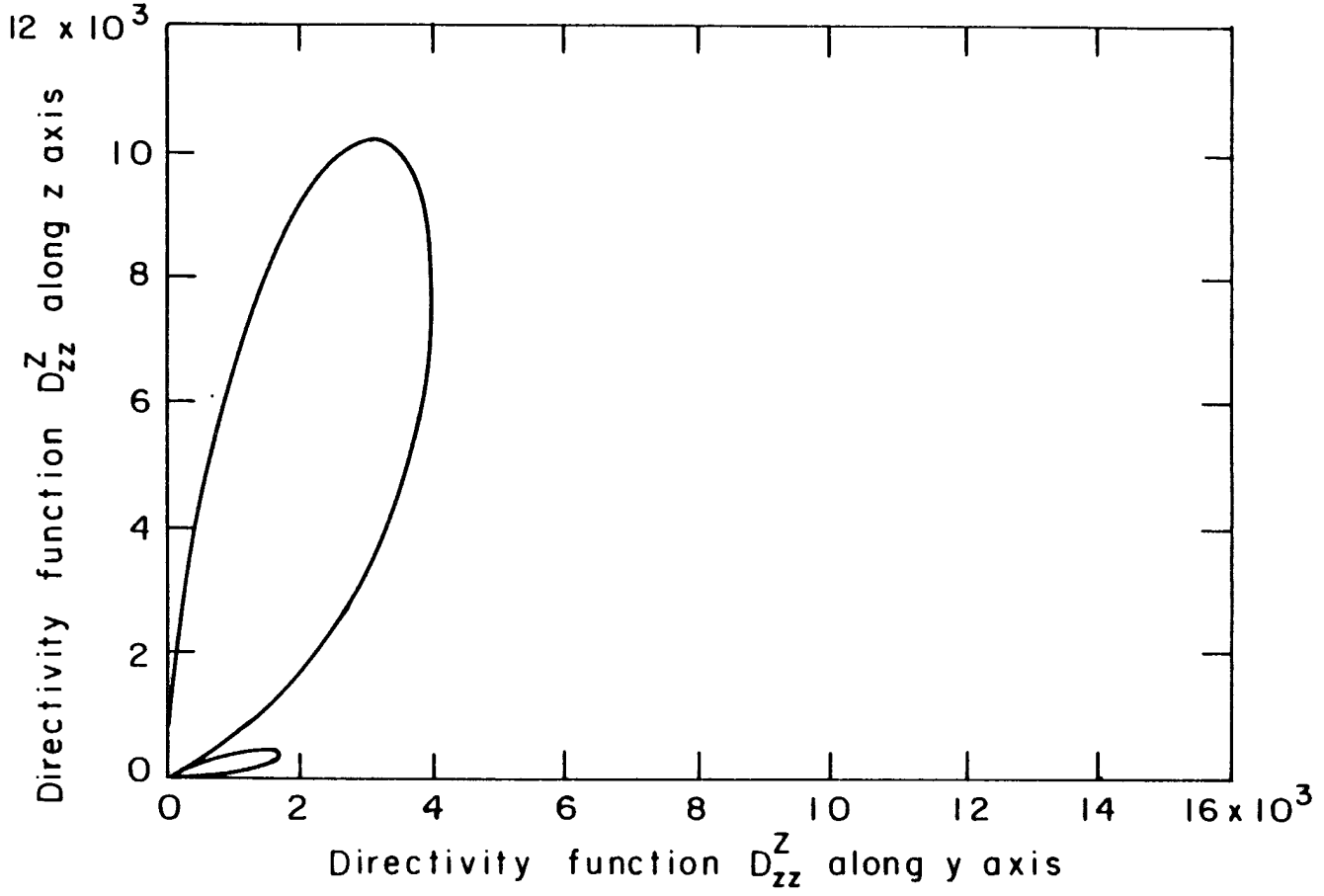

Fig. 21 Polar diagram for directivity function D_{zz}^{Z} of normal stress τ_{zz} at transmitting origin associated with P wave in unidirectional fiberglass epoxy composite at frequency of 0.75 MHz for positive y-z quadrant due to applied point load acting along z-direction.

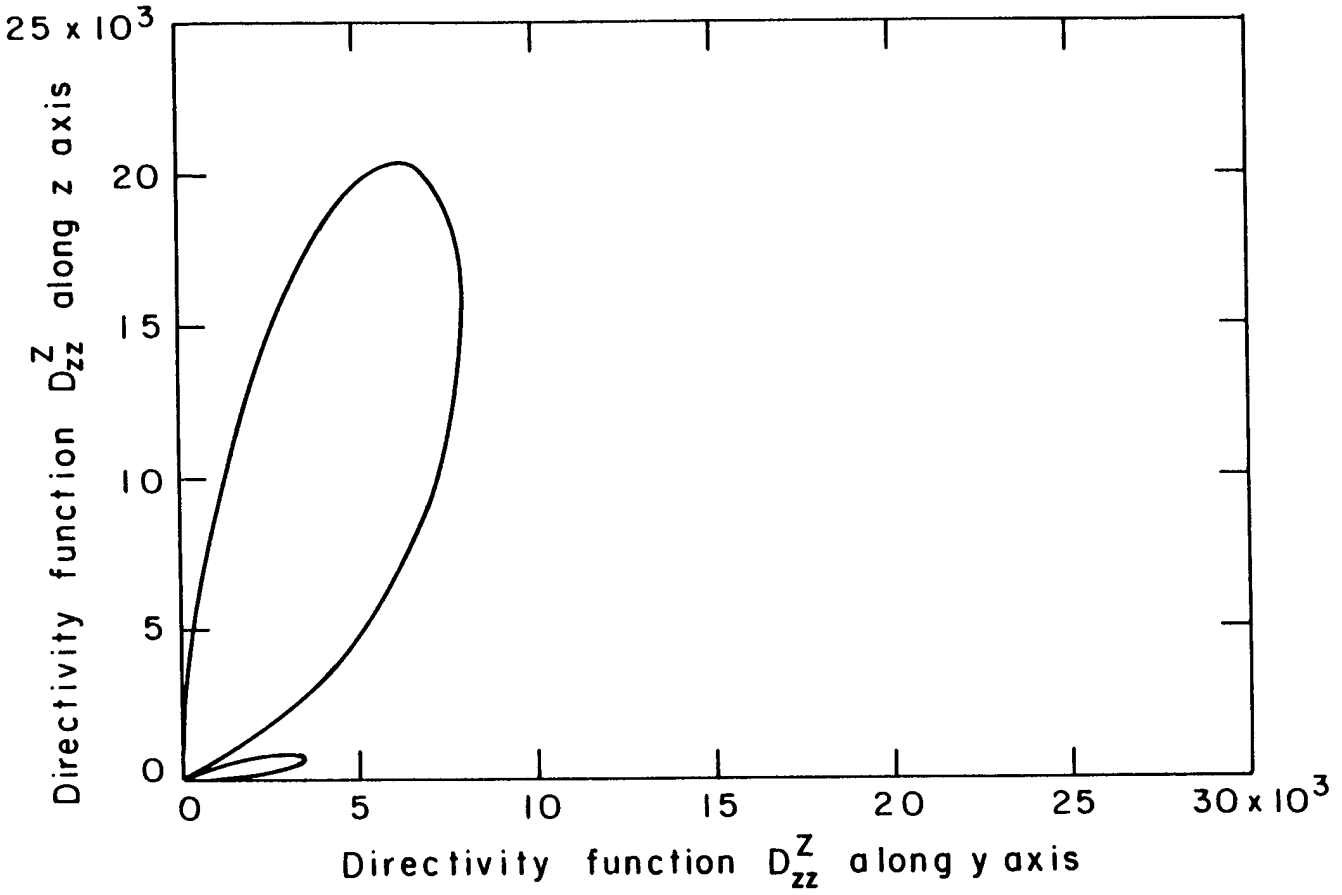

Fig. 22 Polar diagram for directivity function D_{zz}^{z} of normal stress τ_{zz} at transmitting origin associated with P wave in unidirectional fiberglass epoxy composite at frequency of 1.50 MHz for positive y-z quadrant due to applied point load acting along z-direction.

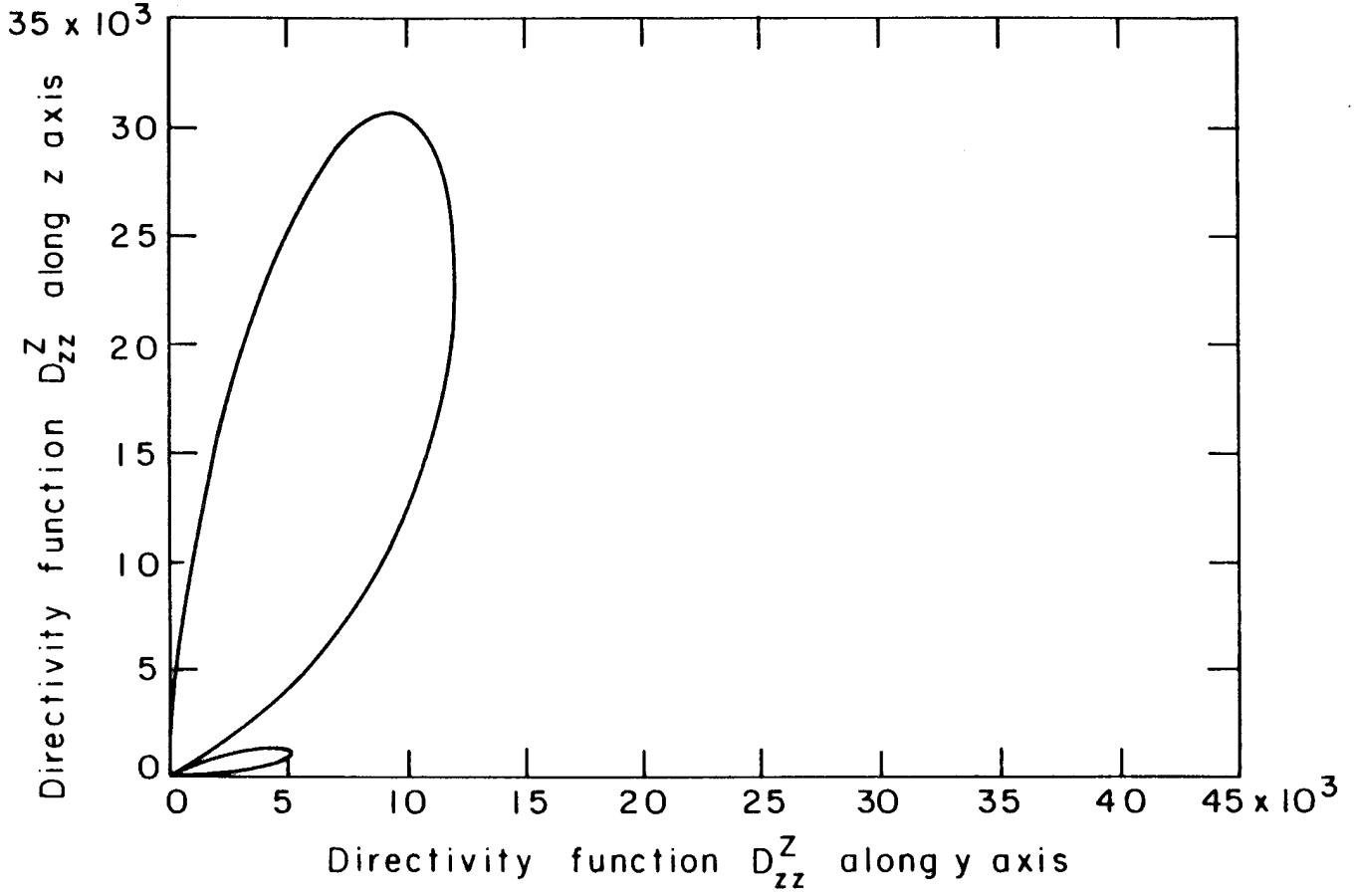

Fig. 23 Polar diagram for directivity function D^{Z}_{zz} of normal stress τ_{zz} at transmitting origin associated with P wave in unidirectional fiberglass epoxy composite at frequency of 2.25 MHz for positive y-z quadrant due to applied point load acting along z-direction.

NASA
National Aeronautics and Space Administration

Report Documentation Page

1. Report No.	2. Government Accession No.	3. Recipient's Catalog No.
NASA CR-4162		

4. Title and Subtitle	5. Report Date
Acousto-Ultrasonic Input-Output Characterization of Unidirectional Fiber Composite Plate by P Waves	July 1988
	6. Performing Organization Code

7. Author(s)	8. Performing Organization Report No.
Peter Liao and James H. Williams, Jr.	None (E-4208)
	10. Work Unit No. 506-43-11

9. Performing Organization Name and Address	11. Contract or Grant No.
Massachusetts Institute of Technology Dept. of Mechanical Engineering Cambridge, Massachusetts 02139	NAG3-328
	13. Type of Report and Period Covered Contractor Report Final

12. Sponsoring Agency Name and Address	14. Sponsoring Agency Code
National Aeronautics and Space Administration Lewis Research Center Cleveland, Ohio 44135-3191	

15. Supplementary Notes

Project Manager, Harold E. Kautz, Structures Division, NASA Lewis Research Center.

16. Abstract

The single reflection problem for an incident P wave at a stress-free plane boundary in a semi-infinite transversely isotropic medium whose isotropic plane is parallel to the plane boundary is analyzed. It is found that an obliquely incident P wave results in a reflected P wave and a reflected SV wave. The delay time for propagation between the transmitting and the receiving transducers is computed as if the P waves were propagating in an infinite half space. The displacements associated with the P waves in the plate and which may be detected by a noncontact NDE receiving transducer are approximated by an asymptotic solution for an infinite transversely isotropic medium subjected to a harmonic point load.

17. Key Words (Suggested by Author(s))	18. Distribution Statement
Acousto-ultrasonics; Anisotropic media; Ultrasonics; Nondestructive evaluation; Stress wave factor; Wave propagation	Unclassified - Unlimited Subject Category 38

19. Security Classif. (of this report)	20. Security Classif. (of this page)	21. No of pages	22. Price*
Unclassified	Unclassified	80	A05

NASA FORM 1626 OCT 86

*For sale by the National Technical Information Service, Springfield, Virginia 22161

NASA-Langley, 1988